

See discussions, stats, and author profiles for this publication at: <https://www.researchgate.net/publication/342721488>

# Intrinsic network architecture predicts the effects elicited by intracranial electrical stimulation of the human brain

Article in *Nature Human Behaviour* · July 2020

DOI: 10.1038/s41562-020-0910-1

CITATIONS

0

READS

60

9 authors, including:



**Kieran Fox**

Stanford University

51 PUBLICATIONS 2,359 CITATIONS

[SEE PROFILE](#)



**Sori Baek**

Princeton University

7 PUBLICATIONS 6 CITATIONS

[SEE PROFILE](#)



**Omri Raccah**

New York University

7 PUBLICATIONS 18 CITATIONS

[SEE PROFILE](#)



**Brett L Foster**

Baylor College of Medicine

56 PUBLICATIONS 1,552 CITATIONS

[SEE PROFILE](#)

Some of the authors of this publication are also working on these related projects:



The Oxford Handbook of Spontaneous Thought: Mind-wandering, Creativity, Dreaming, and Clinical Contexts [View project](#)



C3-Brain (2013 - 2030) [View project](#)



# Intrinsic network architecture predicts the effects elicited by intracranial electrical stimulation of the human brain

Kieran C. R. Fox<sup>1,2,6</sup>  , Lin Shi<sup>1,3,6</sup> , Sori Baek<sup>1</sup> , Omri Racah<sup>1</sup> , Brett L. Foster<sup>4</sup> , Srijani Saha<sup>1</sup>, Daniel S. Margulies<sup>5</sup>, Aaron Kucyi<sup>1</sup>  and Josef Parvizi<sup>1</sup>  

**Intracranial electrical stimulation (iES) of the human brain has long been known to elicit a remarkable variety of perceptual, motor and cognitive effects, but the functional-anatomical basis of this heterogeneity remains poorly understood. We conducted a whole-brain mapping of iES-elicited effects, collecting first-person reports following iES at 1,537 cortical sites in 67 participants implanted with intracranial electrodes. We found that intrinsic network membership and the principal gradient of functional connectivity strongly predicted the type and frequency of iES-elicited effects in a given brain region. While iES in unimodal brain networks at the base of the cortical hierarchy elicited frequent and simple effects, effects became increasingly rare, heterogeneous and complex in heteromodal and transmodal networks higher in the hierarchy. Our study provides a comprehensive exploration of the relationship between the hierarchical organization of intrinsic functional networks and the causal modulation of human behaviour and experience with iES.**

For more than a century, intracranial electrical stimulation (iES) of brain tissue in awake neurosurgical patients has been known to elicit a remarkable variety of perceptual, motor, affective and cognitive effects, including somatosensations, visual hallucinations, emotions and memories<sup>1</sup>. Pioneering work by past investigators, particularly the legendary Wilder Penfield, laid the foundation for a high-level understanding of iES effects throughout the human brain<sup>2,3</sup>. We aimed to build on this work by creating a comprehensive, whole-brain mapping of iES responses, then integrating the global pattern of iES effects with emerging models of the brain's large-scale cortical organization<sup>4</sup>. Non-invasive neuroimaging has shown that the brain is organized as a complex mosaic of interlaced, intrinsic functional-anatomical networks<sup>5,6</sup>, and there is growing awareness that iES leads to downstream electrophysiological effects that depend on the network connectivity profile of the region being stimulated<sup>7–13</sup>. However, it remains to be determined whether there is any systematic relationship between the intrinsic functional architecture of the brain and the frequency or type of first-person reports elicited by iES. Beyond addressing fundamental questions about the functional organization of the human cortex, further work bridging iES, neuroimaging and first-person reports might also provide relevant information that could help address the challenges facing ongoing research using chronically implanted iES devices to modulate mood in intractable neuropsychiatric conditions<sup>14–16</sup>.

Towards these aims, we sought to provide a comprehensive map of iES effects across all human intrinsic brain networks, integrating first-person reports, invasive brain stimulation and existing atlases of non-invasive neuroimaging network data drawn from large, representative samples<sup>5,17,18</sup>. Our goals were to: contribute rare causal data to higher-order models of cortical organization<sup>4</sup>; extend

knowledge of the relationship between network properties and the electrophysiological effects of iES<sup>7–13</sup> into the domain of human behaviour and subjective experience; and inform emerging clinical interventions<sup>16</sup>.

## Results

### Elicitation rate differs markedly across intrinsic brain networks.

First, we marshalled evidence from iES functional mapping procedures conducted by a neurologist (J.P.) over the past 10 years at the Stanford University Medical Center. Patients with intractable (that is, medication-resistant) epilepsy are often implanted with intracranial electrodes to precisely determine the source of their seizures before neurosurgical resection of the pathological tissue. Sequential stimulation of electrode contacts (so-called functional mapping) with iES is a standard and safe<sup>19</sup> procedure with great clinical utility, resulting in marked improvements in patient outcomes following neurosurgery<sup>20</sup>. The careful recording of any effects elicited by iES is a routine part of the functional mapping procedure. Over time, this yields rich datasets amenable to exploration of the functional characteristics of particular brain regions<sup>21,22</sup> or testing of specific hypotheses, as in the present study.

Ultimately, we analysed information from 1,537 unique electrode sites implanted in 67 patients with focal epilepsy undergoing pre-surgical intracranial electroencephalography (iEEG) monitoring. IES was performed by an experienced neurologist (J.P.) using parameters typical in functional mapping sessions (macroelectrodes; 50 Hz; 2–10 mA current; 200–300  $\mu$ s pulse width; administered during task-free resting states; see Methods). Electrodes showing pathological epileptiform activity were identified by the attending neurology team and were excluded from analysis; all

<sup>1</sup>Stanford Human Intracranial Cognitive Electrophysiology Program, Department of Neurology and Neurological Sciences, Stanford University, Stanford, CA, USA. <sup>2</sup>School of Medicine, Stanford University, Stanford, CA, USA. <sup>3</sup>Department of Neurosurgery, Beijing Tiantan Hospital, Capital Medical University, Beijing, China. <sup>4</sup>Departments of Neurosurgery and Neuroscience, Baylor College of Medicine, Houston, TX, USA. <sup>5</sup>Centre National de la Recherche Scientifique (CNRS), UMR 7225, Frontlab, Institut du Cerveau et de la Moelle Épinrière, Paris, France. <sup>6</sup>These authors contributed equally: Kieran C. R. Fox, Lin Shi. ✉e-mail: [kcrfox@stanford.edu](mailto:kcrfox@stanford.edu); [jparvizi@stanford.edu](mailto:jparvizi@stanford.edu)

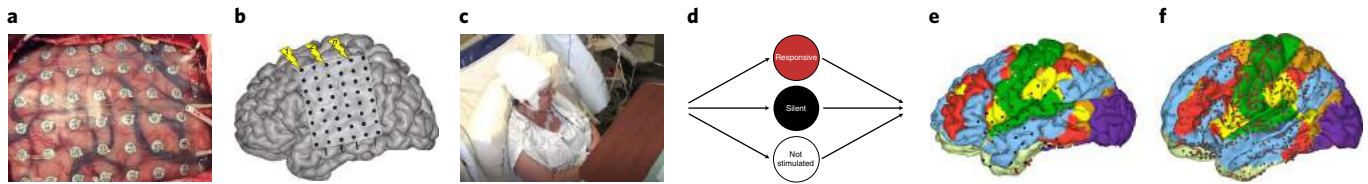


**Fig. 1 | Experimental protocol: intracranial electrode implantation, iES functional mapping, and data coding and aggregation.** **a**, First, neurosurgeons implanted intracranial electrode arrays (based strictly on clinical criteria), to precisely record from and stimulate the brains of patients with intractable epilepsy. **b**, During so-called functional mapping sessions, as many electrodes as possible were sequentially stimulated using brief pulses of electrical current. In an ideal session, all electrodes were stimulated, but in practice iES sessions were limited by both practical (for example, time constraints) and clinical (for example, seizure onset) considerations. **c**, Following each stimulation, the patient reported on whether they detected any change in either their body (for example, somatosensations or motor movements) or aspects of their subjective experience (for example, changes in visual perception or emotions). If no change was noticed, the current amplitude was gradually increased (within safe limits<sup>32</sup>) over subsequent stimulations at the same electrode. **d**, Based on patients' reports, each electrode was classified as either responsive (some change was detected and reported), silent (no change, even after repeated, higher-amplitude iES) or not stimulated (electrode not stimulated during functional mapping session due to one of the aforementioned constraints). Responsive electrodes were further subcategorized by the type of effect elicited (for example, visual, emotional, etc.). **e**, All electrodes were automatically assigned to a particular intrinsic brain network using a well-validated algorithm<sup>23</sup>, implemented at the level of patients' individual neuroanatomy (that is, participant-specific space). **f**, Finally, data from all patients were aggregated in standard MNI space for group-level analysis, and the ratio of responsive to silent electrodes was determined for each network.

of the results reported here are therefore from non-epileptic sites within the human brain. Following iES, each electrode site was coded, using a binary scheme, as either silent or responsive. At silent sites, iES elicited no noticeable effect, even at high current amplitude (importantly, in our clinical practice, if stimulation does not yield any effect, we increase the current until the maximum safe limits are reached; Fig. 1). At responsive sites, iES led to a reportable change in experience according to the patient (including objectively verifiable effects, such as motor movements, as well as subjective experiences such as changes in perception or emotion).

To control for demand characteristics and false positive reports, a total of 116 sham stimulations were also delivered ( $M=1.73$  per patient). Only 11 led to false positive reports (the remaining 105 shams yielding true negatives)—an overall false positive rate of just 9.5%. Notably, false positives were restricted to just seven patients (~10% of our sample), and a single patient contributed nearly half of all false positive reports identified (patient 66 committed five type I errors). No other patient committed more than a single type I error, even after numerous sham stimulations.

After excluding false positives, we determined the network membership of each stimulation site. Each electrode was automatically assigned to the nearest intrinsic brain network using a population-level atlas<sup>23</sup> implemented in subject-specific (native) brain space. The ratio of silent to responsive sites across all patients was aggregated to derive an overall elicitation rate for each network (Fig. 1 and Methods). We found marked differences throughout the brain, with high elicitation rates in somatomotor (55%) and visual networks (52%), intermediate rates in the salience (50%), dorsal attention (39%) and frontoparietal networks (32%), and low rates in the limbic (24%) and default networks (21%) (Fig. 2, Supplementary Fig. 1 and Table 1). We observed equivalent trends using a 17-network parcellation (Fig. 3 and Table 2). Network membership is already known to be an important factor in predicting the downstream electrophysiological sequelae of iES<sup>8–12</sup>; our findings provide detailed evidence that network membership is also a major determinant of the effects that iES has on human behaviour and experience. Moreover, far from being merely an emergent, average pattern, these trends were evident even at the individual level in patients with electrodes spanning multiple networks (Fig. 4; all participants in Supplementary Information).

Because previous research has shown differences in the effects elicited by iES in the left versus right hemispheres<sup>21,24</sup>, we also explored whether any hemispheric asymmetries were present in our

dataset. We found a small but significant difference in overall elicitation rate between the left (34.6%) and right (43.4%) hemispheres of the brain ( $t(1,535)=3.279$ ;  $P=0.001$ ;  $d=0.18$ ; 95% confidence interval (95% CI)=0.07–0.29). Post-hoc  $t$ -tests showed that this difference was driven by higher elicitation rates in the somatomotor and salience networks, as well as a lower elicitation rate in the visual network, of the right hemisphere. While interhemispheric differences between other networks were not statistically significant, elicitation rates were consistently higher in the right hemisphere (full results in Extended Data Fig. 1).

To ensure the reliability of our central finding of differential rates across networks, we conducted several supplemental estimations of networks' elicitation rates, using: (1) only electrodes on the lateral surface of the brain; (2) only electrodes from the medial surface; (3) discovery versus replication samples each including a random half of participants based on a 50/50 split; and (4) a randomly selected half of all electrodes, averaged over 100 iterations (see Methods). All supplemental estimates of network elicitation rates correlated highly with our full dataset (seven-network parcellation: all  $r$  values  $\geq 0.79$ ; Supplementary Table 1; 17-network parcellation: all  $r$  values  $\geq 0.74$ ; Supplementary Table 2), indicating that our estimated elicitation rates were highly reliable.

**Elicitation rate closely tracks the principal gradient in intrinsic network functional connectivity.** Next, we asked whether this pattern showed a relationship with large-scale cortical gradients across these networks. Neuroscientists have long proposed that the cerebral cortex is organized along a functional–anatomical gradient, with concrete, unimodal sensory processing at one end of the hierarchy and more abstract, transmodal cognition at the other<sup>25–28</sup>. Patterns of variance in the functional connectivity within and between intrinsic brain networks exhibit such a gradient, anchored at one end by unimodal visual and somatomotor networks with low variability, and at the other by highly variable, transmodal default and limbic networks<sup>17</sup>. Hierarchical gradients provide a unifying framework that promises to shed considerable light on the global relationship between the anatomical organization and functional properties of the cerebral cortex<sup>4</sup>, but the effects elicited by iES have yet to be integrated with these models. Noticing the correspondence between our findings and the global hierarchy previously described by the principal gradient in functional connectivity<sup>17</sup>, we correlated elicitation rates with the mean principal gradient value of each network as estimated by intrinsic functional connectivity

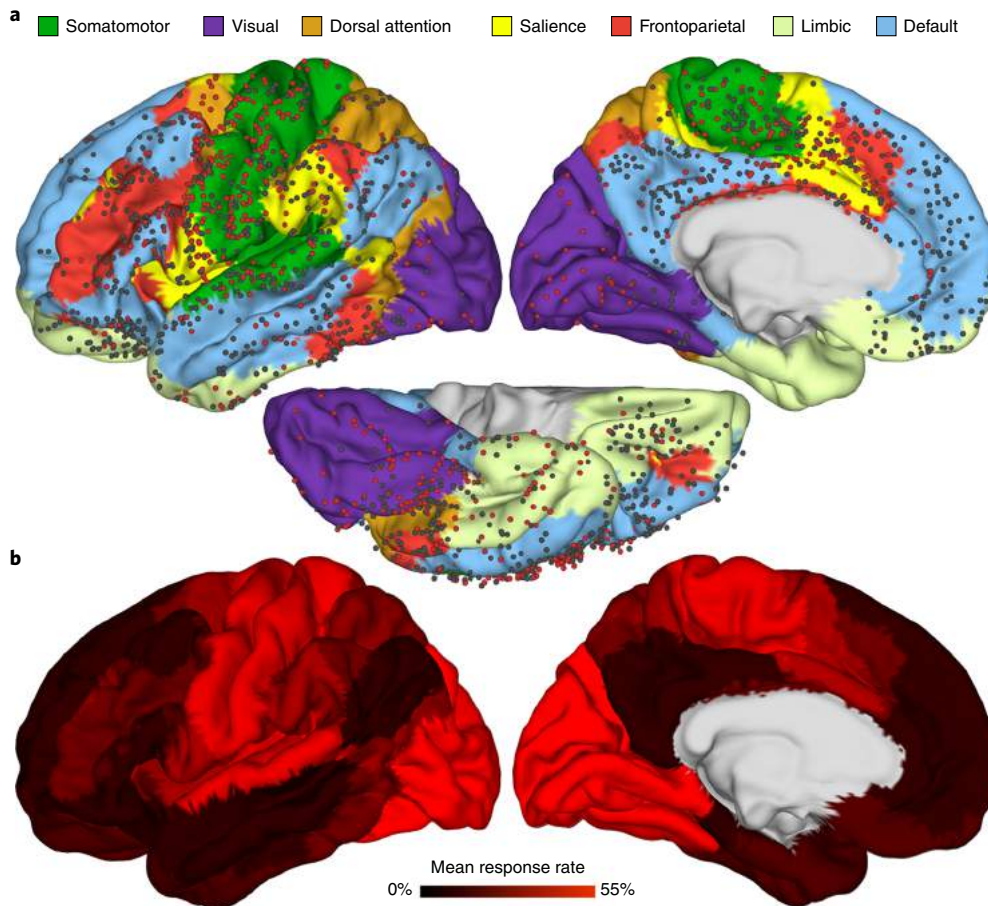


**Fig. 2 | Elicitation rate of iES varies markedly across intrinsic networks (seven-network parcellation).** **a,b**, Aggregated data from all 67 patients in standard brain space overlaid on a seven-network parcellation of the cerebral cortex. In **a**, red circles indicate responsive electrodes, where stimulation elicited an effect, and black circles indicate null electrodes, where no effects were elicited even with repeated high-amplitude stimulation. In **b**, averaging of the response rate for each network shows that the mean elicitation rate varies markedly but gradually (that is, linearly) across networks: somatomotor and visual networks show the highest response rates; default and limbic networks show the lowest; and other networks show intermediate rates (Table 1). Nearly identical trends were observed using a finer 17-network parcellation (Fig. 3 and Table 2).

**Table 1 | Elicitation rates and current thresholds for the seven-network parcellation**

Network	Electrodes			Current thresholds (mA)	
	Total	Responsive	Silent	Mean minimum elicitation threshold ( $\pm$ s.d.)	Mean maximum quiescence threshold ( $\pm$ s.d.)
Somatomotor	291	159 (54.6%)	132 (45.4%)	4.72 (1.80)	6.67 (2.15)
Visual	182	94 (51.7%)	88 (48.3%)	4.16 (2.16)	6.72 (1.45)
Dorsal attention	71	28 (39.4%)	43 (60.6%)	5.50 (2.38)	7.95 (2.24)
Salience	210	104 (49.5%)	106 (50.5%)	4.97 (1.76)	6.32 (1.92)
Frontoparietal	169	54 (32.0%)	115 (68.0%)	4.41 (1.89)	6.62 (1.99)
Limbic	195	47 (24.1%)	148 (75.9%)	4.41 (1.40)	5.82 (2.11)
Default	419	87 (20.8%)	332 (79.2%)	4.88 (2.09)	6.61 (2.02)
Totals and means	1,537	573 (37.3%)	964 (62.7%)	4.68 (1.94)	6.54 (2.04)

variance in the functional MRI (fMRI) blood oxygen level-dependent signal (see Methods). We found striking evidence that elicitation rate closely tracks principal gradient values (seven-network parcellation:  $r(5)=0.96$ ;  $P<0.001$ ; 95% CI=0.75–0.99; Fig. 5a and Extended Data Fig. 2; 17-network parcellation:  $r(15)=0.82$ ;  $P<0.001$ ; 95% CI=0.56–0.93; Fig. 5c and Extended Data Fig. 3),

with unimodal networks showing the highest elicitation rates and transmodal networks the lowest. This relationship also held for all of our supplemental estimates of network elicitation rate (Extended Data Figs. 2 and 3).

To confirm this relationship independent of network parcellations, and across the gradient's full range, we extracted principal

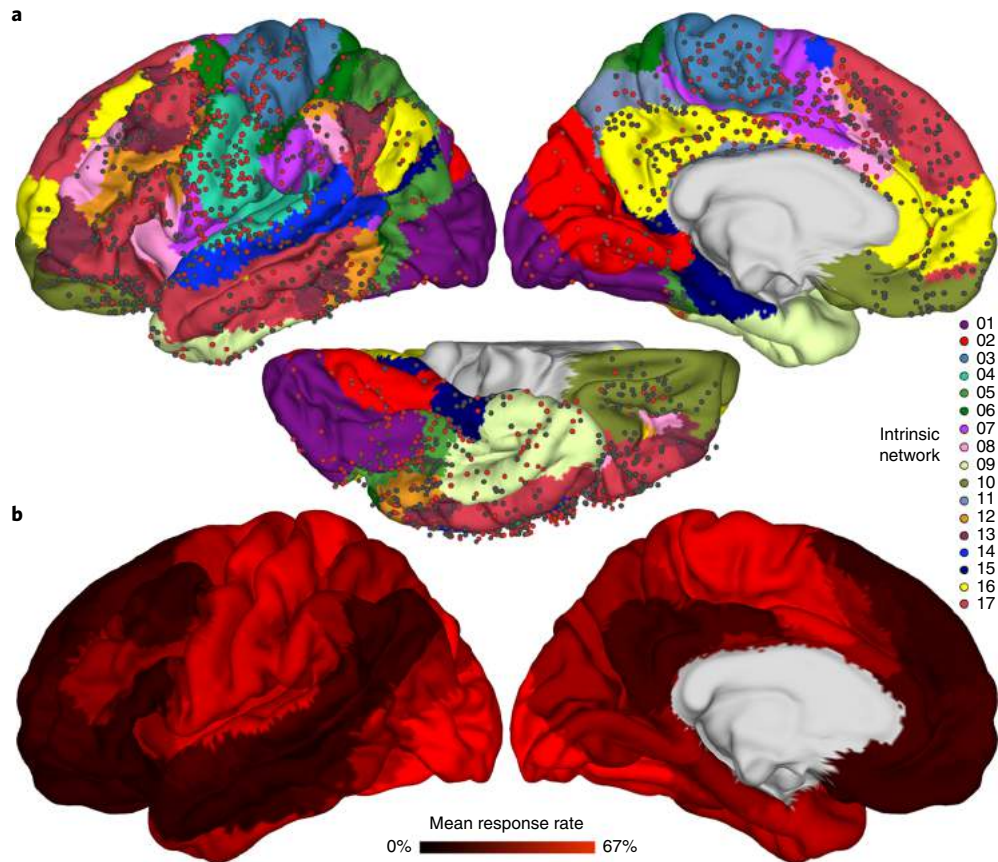


**Fig. 3 | Elicitation rate of iES varies markedly across intrinsic networks (17-network parcellation).** **a,b**, Aggregated data from all 67 patients in standard brain space overlaid on a 17-network parcellation of the cerebral cortex. **a**, Electrodes are colour coded as in Fig. 2. **b**, As in the seven-network parcellation of the brain (Fig. 2), average response rates for each network vary linearly across a finer-scale 17-network parcellation of the cortical surface.

**Table 2 | Elicitation rates and current thresholds for the 17-network parcellation**

Network	Electrodes			Current thresholds (mA)	
	Total	Responsive	Silent	Mean minimum elicitation threshold ( $\pm$ s.d.)	Mean maximum quiescence threshold ( $\pm$ s.d.)
01	52	35 (67.3%)	17 (32.7%)	4.21 (2.42)	6.44 (1.42)
02	102	44 (43.1%)	58 (56.9%)	3.83 (2.15)	6.61 (1.37)
03	175	103 (58.9%)	72 (41.1%)	4.39 (1.75)	6.31 (2.16)
04	78	42 (53.9%)	36 (46.1%)	5.34 (1.78)	7.22 (1.88)
05	47	21 (44.7%)	26 (55.3%)	5.05 (2.20)	8.41 (1.59)
06	40	16 (40.0%)	24 (60.0%)	5.69 (1.25)	7.17 (2.41)
07	156	85 (54.5%)	71 (45.5%)	5.07 (1.77)	6.34 (1.81)
08	97	37 (38.1%)	60 (61.9%)	4.61 (2.08)	6.11 (1.72)
09	49	24 (49.0%)	25 (51.0%)	4.25 (1.15)	6.00 (1.98)
10	149	24 (16.1%)	125 (83.9%)	4.81 (1.78)	5.71 (2.14)
11	54	21 (38.9%)	33 (61.1%)	4.86 (1.88)	6.54 (2.64)
12	59	23 (39.0%)	36 (61.0%)	4.14 (1.55)	7.06 (2.15)
13	71	14 (19.7%)	57 (80.3%)	5.69 (2.59)	6.63 (1.93)
14	40	9 (22.5%)	31 (77.5%)	6.11 (2.20)	7.96 (2.13)
15	35	12 (34.3%)	23 (65.7%)	4.38 (0.87)	6.76 (1.89)
16	173	36 (20.8%)	137 (79.2%)	4.38 (1.95)	6.37 (2.12)
17	160	27 (16.9%)	133 (83.1%)	4.88 (2.31)	6.78 (1.87)
<b>Totals and means</b>	<b>1,537</b>	<b>573 (37.3%)</b>	<b>964 (62.7%)</b>	<b>4.68 (1.94)</b>	<b>6.54 (2.04)</b>

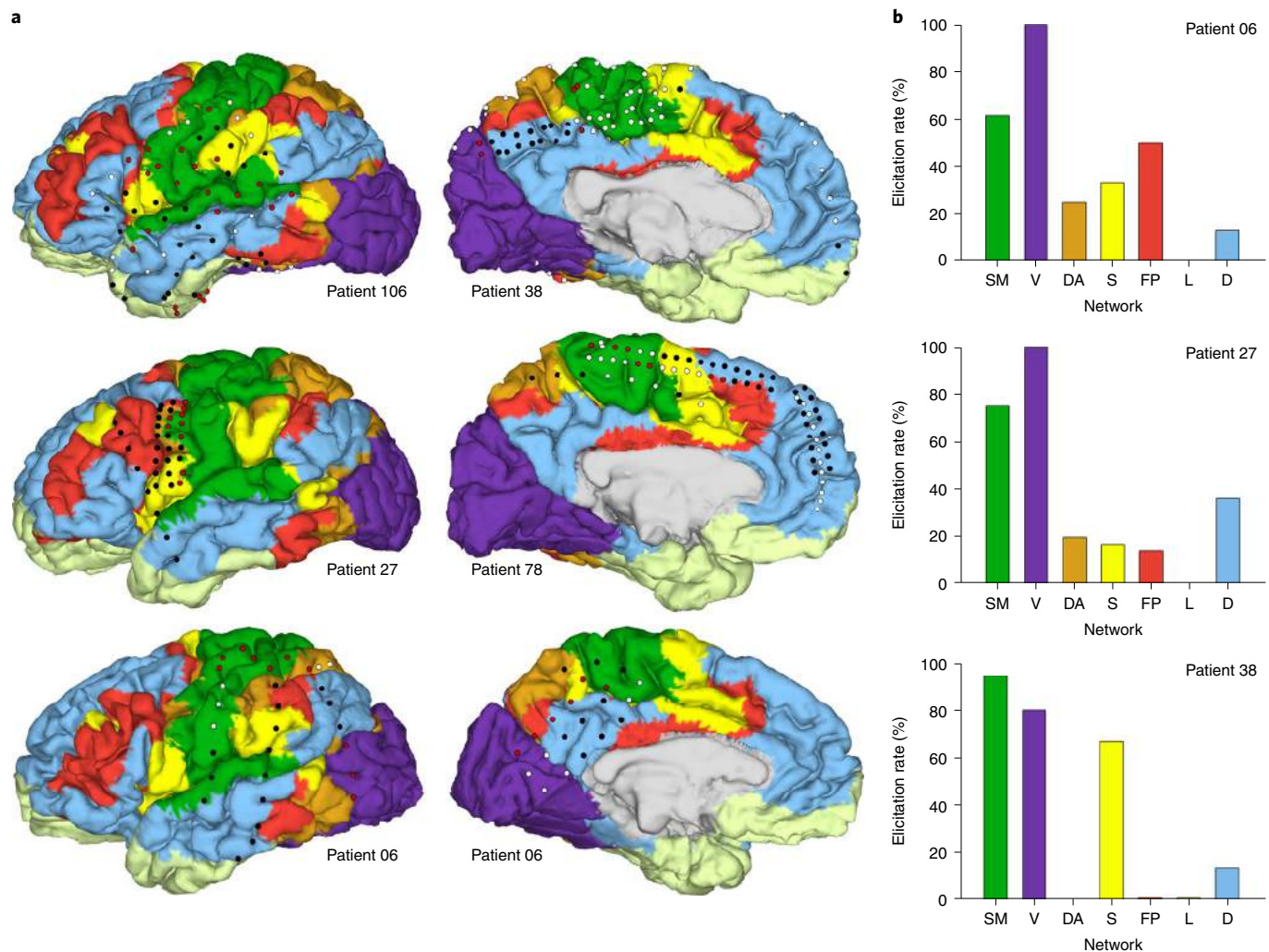


**Fig. 4 | Network-specific elicitation patterns are present at the level of individual patients.** **a**, Responsive (red) and silent (black) sites in the brains of six patients with electrodes spanning multiple networks. Even at the level of individual patients' neuroanatomy, iES in unimodal networks was clearly more likely to elicit effects. White circles indicate electrodes where iES was not administered. Networks are colour coded as in Fig. 2. **b**, Network-specific elicitation rates from three patients where iES was administered at a large number of electrodes (spanning at least six of the seven intrinsic networks). Despite heterogeneity at the individual level, the general trend in elicitation rates was apparent in patients with many stimulated electrodes. Network elicitation rates were derived from 41, 45 and 50 electrodes, respectively, for the top, middle and bottom panels. Absence of a histogram bar indicates that no data were available for this network for a given patient. D, default; DA, dorsal attention; FP, frontoparietal; L, limbic; S, salience; SM, somatomotor; V, visual.

gradient values at each vertex in cortical surface space where iES had been administered. We used mixed-effects logistic regression to relate principal gradient value (fixed effect) to the binary coding of electrode sites (silent/responsive) as the dependent variable, modelling patient as a random effect (see Methods). We found that vertex-level principal gradient values showed a significant relationship with our coding of iES effects ( $\chi^2(55)=394.565$ ;  $P<0.0001$ ; Supplementary Tables 3 and 4), with silent electrode sites associated, as expected, with higher principal gradient values. Together, these data indicate that the fMRI intrinsic functional connectivity profile of a given brain region is a powerful predictor of whether or not effects will be induced with iES—an entirely independent modality.

**Elicited effects become more heterogeneous ascending the cortical hierarchy.** We then undertook a detailed investigation of the specific quality of the effects elicited throughout the brain. In line with our previous work<sup>21</sup>, we employed broad, data-driven categories to classify patients' reports at every responsive electrode

where iES elicited some change. Ultimately, eight categories were employed: (1) somatomotor; (2) visual; (3) olfactory; (4) vestibular; (5) emotional; (6) language; (7) memory; and (8) physiological. Importantly, no type of effect was excluded a priori: the absence of certain categories of effects reported in previous research<sup>29</sup> probably reflects the rarity of certain types of effects, which were not observed even in our comparatively large sample (for further details, see Methods). Classified results were then pooled to yield an estimate of the prevalence of each effect type for each brain network (Extended Data Figs. 4 and 5).

We found that the network membership of a stimulated electrode significantly predicted the category of elicited effect (seven-network parcellation:  $\lambda=0.312$ ;  $P<0.001$ ; 17-network parcellation:  $\lambda=0.364$ ;  $P<0.001$ ), indicating that, as expected<sup>29</sup>, stimulation of different networks yields widely divergent effects. However, we also found evidence that the heterogeneity of effect categories elicited within a given network correlated with the network's principal gradient value (seven-network parcellation:  $r(5)=0.77$ ;  $P=0.044$ ; 95% CI=0.04–0.96; Fig. 5b; 17-network

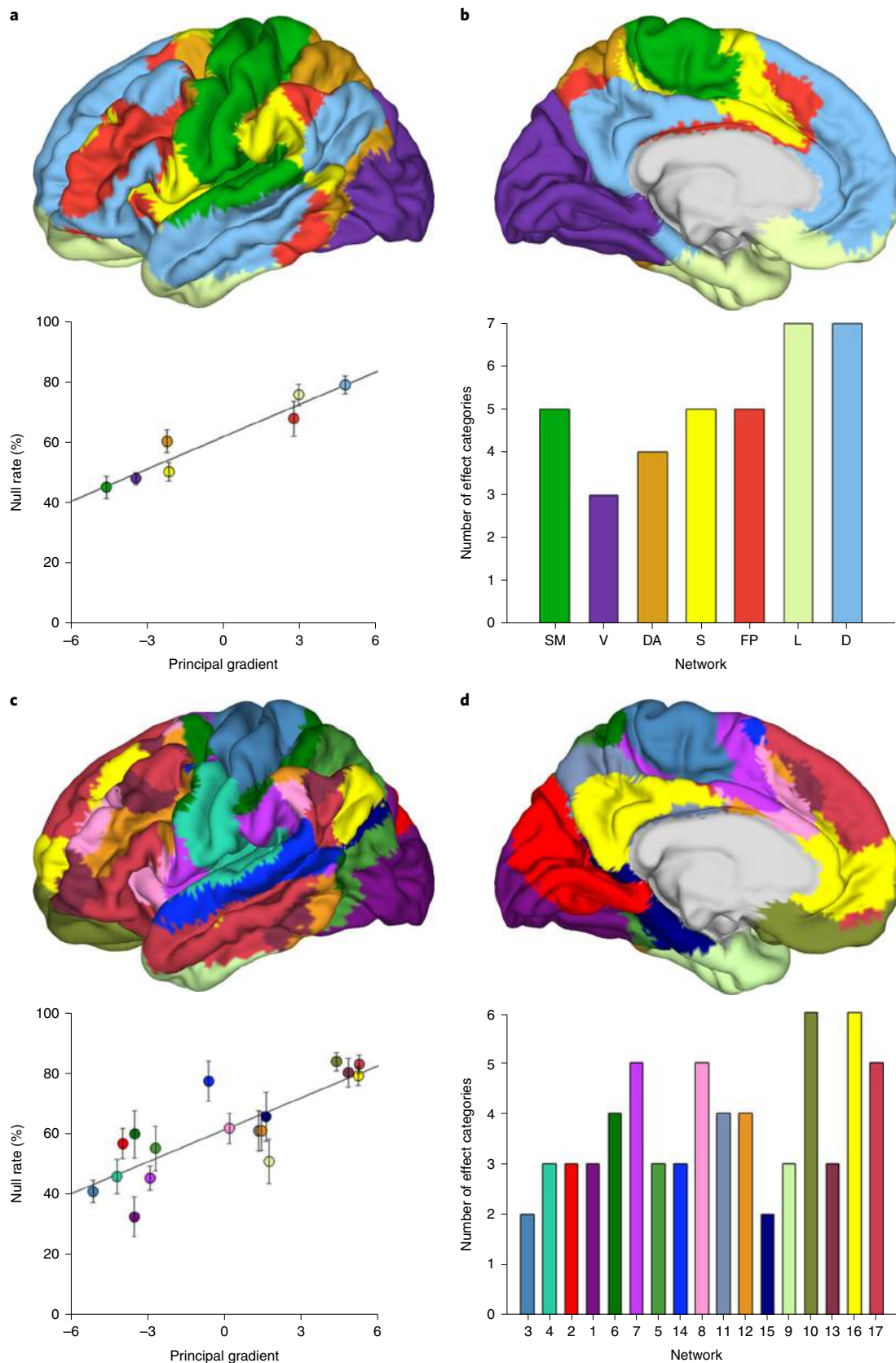


**Fig. 5 | Relationships between network elicitation rates, position in the principal gradient hierarchy and the diversity of elicited effects. a,c.** The principal gradient of functional connectivity<sup>17</sup> predicts the rate of effects elicited by iES in both seven-network (**a**) ( $r=0.96$ ) and 17-network (**c**) ( $r=0.82$ ) parcellations of human cerebral cortex. **b,d.** Despite fewer effects elicited overall, ascending along the cortical hierarchy, a greater diversity of effects is elicited for both seven-network (**b**) and 17-network (**d**) parcellations. Network data in all panels are arranged in order of increasing principal gradient value. Error bars indicate s.e.m.

parcellation:  $r(15)=0.51$ ;  $P=0.035$ ; 95% CI=0.04–0.80; Fig. 5d). These significant relationships were observed despite the fact that under the null hypothesis (that is, diversity of effects is equal across all networks) networks with a larger number of responsive electrodes have a higher probability of exhibiting greater effect diversity (or, equivalently, as the number of responsive electrodes in a given network approaches zero, the probability of observing effects from all eight of our categories diminishes correspondingly). As anticipated, then, when the small number of effects in transmodal networks was accounted for by controlling for the total number of responsive electrodes in each network, the observed associations were amplified (seven-network parcellation: partial  $r(4)=0.84$ ;  $P=0.035$ ; 95% CI=0.09–0.98; 17-network parcellation: partial  $r(14)=0.58$ ;  $P=0.020$ ; 95% CI=0.12–0.84). In other words, networks lower in the hierarchy were dominated by unimodal effects of a single type; for instance, 87.2% of all effects elicited in the visual network were visual in nature and 89.3% of effects elicited in the somatomotor network involved somatosensation or motor output (Extended Data Fig. 4). In contrast, despite showing relatively few effects overall, networks at the top of the hierarchy generally exhibited a wider variety of more complex effects that were rarely, if ever, observed in unimodal networks—including emotions and memory recall (Extended Data Fig. 4; equivalent results using a 17-network parcellation are provided in Extended Data Fig. 5). In summary, our results indicate that both the diversity and complexity of effects scales linearly with the principal gradient.

**Network differences in tissue excitability and white matter density do not explain differential elicitation rates.** Finally, we asked whether variable elicitation rates might be explained by variations in either neurophysiological (tissue excitability) or structural-anatomical (white matter density) features that are also thought to vary across intrinsic networks. The biophysical ramifications of artificially administered electrical currents in human brain tissue remain poorly understood<sup>1,30,31</sup>, so first we asked whether differential elicitation rates might be explained by differential tissue excitability across networks. For each responsive electrode, we identified the minimum current (mA) required to elicit an effect. We then calculated a mean elicitation threshold for each network by averaging these minimum currents for all electrodes within a given network. Although the mean minimum elicitation threshold differed significantly across networks (seven-network parcellation:  $F(6,530)=2.753$ ;  $P=0.012$ ; partial  $\eta^2=0.030$ ; 90% CI=0.003–0.047; 17-network parcellation:  $F(16,520)=2.473$ ;  $P=0.001$ ; partial  $\eta^2=0.071$ ; 90% CI=0.015–0.080; Tables 1 and 2), effect sizes were small and statistical significance was clearly driven by the large sample. Moreover, variations in network elicitation threshold showed no significant relationship with either elicitation rate (seven-network parcellation:  $r(5)=0.01$ ;  $P=0.986$ ; 95% CI=–0.75–0.76; Bayes factor ( $BF_{01}$ )=3.70; 17-network parcellation:  $r(15)=0.33$ ;  $P=0.201$ ; 95% CI=–0.18–0.70;  $BF_{01}=2.40$ ) or principal gradient value (seven-network parcellation:  $r(5)=0.14$ ;  $P=0.770$ ; 95% CI=–0.69–0.81;  $BF_{01}=3.54$ ; 17-network parcellation:  $r(15)=0.01$ ;  $P=0.964$ ; 95% CI=–0.47–0.49;  $BF_{01}=5.44$ ). These data comprise evidence that there are small variations in tissue excitability across intrinsic brain networks (Tables 1 and 2). However, we found no evidence that these modest variations explain the large differences in effect elicitation; rather, Bayes factors showed moderate evidence in support of the null hypothesis.

Nonetheless, we further sought to ensure that the high rate of null effects in transmodal networks was not due simply to inadequate current delivery. To this end, the maximum delivered current (mA) yielding no effect for every silent electrode was also tabulated, then averaged for each network (see Methods). This mean maximum quiescence threshold provided a measure, for each network, of the average current delivered at electrodes where no effects were ever

reported. For all networks, we found that this threshold exceeded the mean current required to elicit an effect in the same network (that is, null effects were still observed despite higher mean current delivery than at electrodes where iES did elicit effects in the same network) (Tables 1 and 2). Low rates of effect elicitation in transmodal networks therefore cannot be explained by either higher elicitation thresholds or inadequate current delivery in our study: even at high current magnitudes (6–10 mA) that were well above the typical threshold for eliciting effects (4–5 mA) but still within established safe limits<sup>32</sup>, transmodal networks were far less likely to yield effects.

Research suggests that intrinsic connectivity heterogeneity covaries with regional myelin content<sup>33</sup>, providing a plausible anatomical basis for the functional correlations in the fMRI blood oxygen level-dependent signal. Therefore, we next explored whether regional myelination might also be associated with differential elicitation rates across networks. Using publicly available data from the Human Connectome Project<sup>18</sup>, we estimated regional white matter density in each network using the ratio of T1-weighted to T2-weighted MRI signal. However, we found that a network's average white matter density showed no significant relationship with its elicitation rate (seven-network parcellation:  $r(5)=0.13$ ;  $P=0.784$ ; 95% CI=–0.69–0.80;  $BF_{01}=3.56$ ; 17-network parcellation:  $r(15)=0.31$ ;  $P=0.230$ ; 95% CI=–0.20–0.69;  $BF_{01}=2.65$ ), with Bayes factors supporting the null hypothesis.

Together with our assessment of networks' elicitation and quiescence thresholds, these additional null findings provide crucial control analyses that reaffirm the specific importance of the principal gradient in explaining differential elicitation rates. Although differences in tissue excitability or white matter density are logical explanations for the large differences we observed in elicitation rate, our data show that neither offers a statistically significant explanation for our findings, while in both cases Bayesian inference supports the null hypothesis.

## Discussion

Despite more than a century of iES research on the human brain, theoretical understanding of the nature and pattern of elicited effects has remained limited. Our data provide compelling evidence that the effects elicited by iES closely track a functional hierarchical gradient characterized in human cerebral cortex with an entirely independent methodology (fMRI). Although the strength of this relationship might seem surprising, our results are consistent with recent research showing that iEEG intrinsic functional connectivity is powerfully predicted even by Euclidean distance or simple measures of white matter connectivity<sup>13</sup>. Here, however, we showed that simpler neurophysiological or neuroanatomical attributes of brain tissue, such as electrical excitability or myelin concentration, were unable to explain our findings, which were specific to the functional, rather than anatomical, aspects of intrinsic networks. Building on the growing understanding that functional-anatomical network architecture influences the electrophysiological dynamics of iEEG<sup>7–13</sup>, we have extended these investigations into the domain of the motor, perceptual, affective and cognitive effects elicited with iES (Fig. 6).

To summarize, we demonstrated that network membership—more specifically, each network's position along the principal gradient—is a potent predictor of whether or not iES will elicit an effect (Fig. 2); what type of effect will be elicited (Extended Data Figs. 4 and 5); and how heterogeneous the elicited effects will be (Fig. 5). In unimodal brain networks, effects were up to fourfold more frequent (Table 2) and were largely homogenous (Extended Data Figs. 4 and 5). Conversely, effects were relatively rare in transmodal networks but much more diverse. These findings are consistent with extensive previous research. Past work has found that stimulation of networks at the base of the hierarchy yields frequent, homogenous and simple effects such as phosphenes and

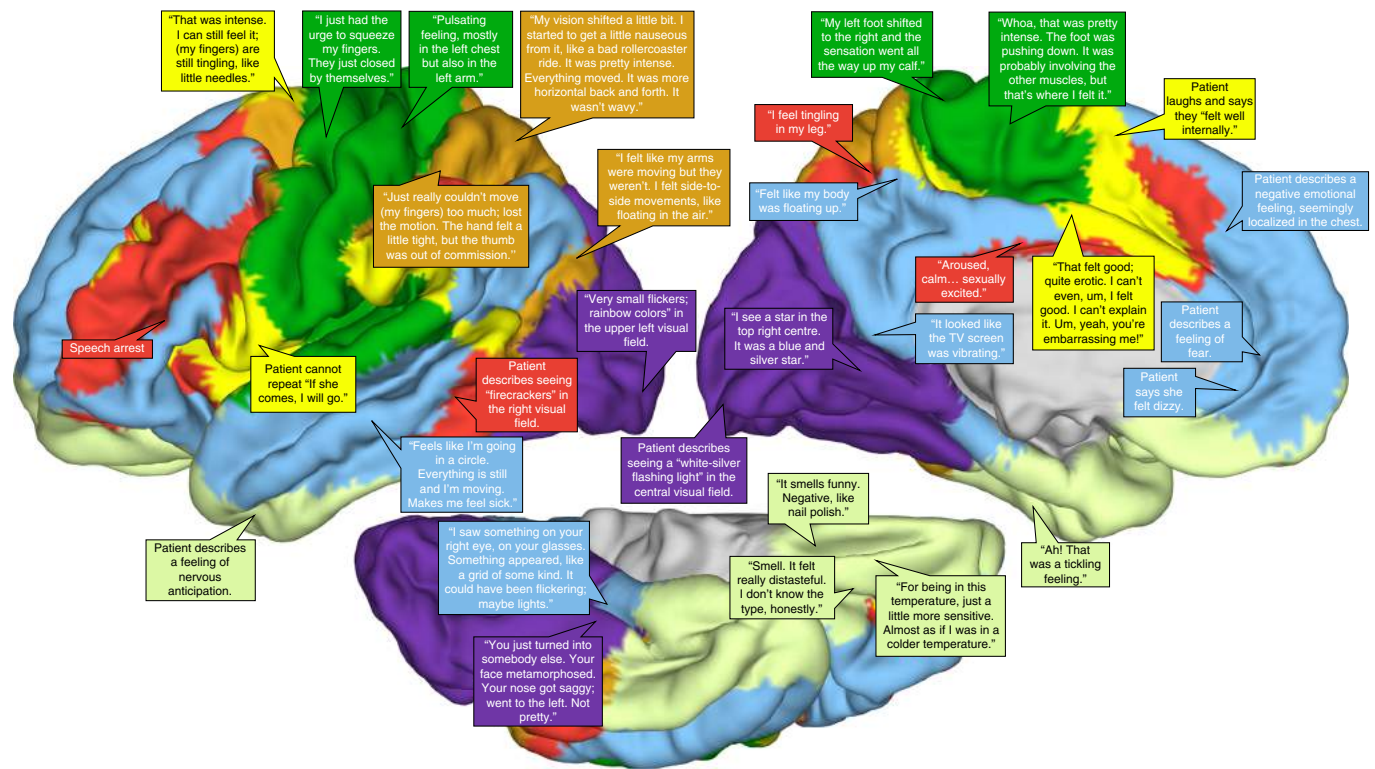


**Fig. 6 | Representative patient reports following iES throughout the brain.** A selection of first-person reports provided by patients following iES throughout all intrinsic networks and brain regions. Text boxes are colour coded to the network in which stimulation yielded the effect, and arrows from text boxes point to the approximate location of each stimulating electrode. While the reports have been accurately linked to the associated network and brain region of the stimulating electrode, the placements are intended to be illustrative; locations are not exact. Text in quotation marks indicates verbatim transcripts of patients' reports. Detailed discussions of some of the more striking effects are available in our published case studies<sup>21,22,24,34,92</sup>.

muscle twitches<sup>29</sup>. Higher in the hierarchy, iES yields rare but diverse and complex effects—often, multimodal experiences tinged with affect<sup>21,22,34</sup>. However, we are mindful that our observations did not replicate every type of effect reported in past research (for instance, refs. <sup>35,36</sup>). Moreover, our finding of higher overall elicitation rates in the right hemisphere (Extended Data Fig. 1) is not readily explained, although it is consistent with recent research showing hemispheric asymmetries in the quality of iES-elicited effects, including differential patterns of emotional valence following orbitofrontal cortex stimulation<sup>21</sup> and asymmetric changes in face perception following stimulation of the fusiform gyrus<sup>24,37</sup>. We believe that our observations should be replicated before being inducted into an already vast and contentious literature on functional-anatomical hemispheric asymmetry<sup>38</sup>.

In addition to the finding that transmodal networks yielded fewer and more diverse effects, it is notable that many effects elicited in transmodal networks were preferentially located near boundaries with other networks. For instance, in the default network, effects in the core of the medial prefrontal cortex were almost entirely absent, but in the dorsomedial prefrontal cortex, some somatomotor effects were apparent along the network's posterior boundary, bordering the frontoparietal and salience networks (Fig. 2a). Transforming electrode locations from individual neuroanatomical space to an averaged intrinsic network template evidently creates some amount of error, especially given that regions at the boundaries of intrinsic networks are less confidently assigned to a given network (that is, in reliability analyses, border regions are less confidently assigned to a given network) (see Figs. 8 and 10 in ref. <sup>5</sup>). This suggests that the comparatively low elicitation rates we observed in transmodal networks might nonetheless actually be overestimates: an improved mapping of network boundaries and better integration with

individual neuroanatomy would probably reveal that transmodal networks are even more quiescent than we report here (with numerous somatomotor and visual effects, for instance, being assigned instead to other networks).

What explains such marked inter-network differences and the relative quiescence of transmodal regions? Probably one crucial factor is that, although the effects of iES are strongest nearest to the stimulating electrode<sup>31</sup>, they are not contained locally: injected current propagates through local circuitry and via active signal transmission along existing connections with other distant areas, and interacts with ongoing electrical activity<sup>1,39,40</sup>. Recent work suggests that iES of functional network hubs (for example, frontoparietal and default regions) leads to rapid attenuation of the delivered current through a hub's many long-distance connections, whereas stimulation of low-degree network nodes (for example, unimodal regions) leads to targeted, more localized activity<sup>8</sup>. Several features specific to unimodal brain regions are also potentially relevant; for instance, unimodal networks tend to contain neurons that are finely tuned to specific perceptual features<sup>41</sup>. Finely tuned neurons in unimodal regions are also typically embedded in cortical columns nested within topographic organizational plans, such that nearby neurons, in both the perpendicular and parallel planes of the cortex, share similar (and similarly specific) tuning properties<sup>42,43</sup>. Prima facie, it seems plausible that localized electrical excitation in tissue with such properties could readily elicit specific perceptual or motoric effects. Furthermore, unimodal neurons and cortical columns are both embedded in hierarchical processing streams with strong feed-forward projections that convey incoming sensory information to higher brain regions for further processing<sup>44</sup>. Such a hierarchical pattern of circuitry seems ideal to amplify the comparatively localized electrical effects exerted by iES. The endogenous amplification

of exogenously induced activity in unimodal cortical sites known to preferentially encode specific and concrete elements of perception and action<sup>45–49</sup> provides a parsimonious explanation for the many simple visual and somatomotor effects we observed. In contrast, virtually all of the aforementioned features are absent or attenuated in transmodal networks<sup>43</sup>. Single neurons in transmodal regions tend to exhibit much more complex patterns of tuning tied to multiple aspects of perception, action and intention. Such non-specific neural coding has been demonstrated in multiple regions that fall within the boundaries of the default and limbic networks, including prefrontal<sup>50–52</sup>, orbitofrontal<sup>52–54</sup>, medial temporal<sup>52,55,56</sup> and posterior cingulate<sup>57</sup> cortices. As others have recently pointed out<sup>58</sup>, eliciting a noticeable change in conscious experience would probably require perturbation of a large proportion and broad selection of neurons characterized by such high-dimensional and non-specific neural representations. The relatively localized<sup>31</sup> (directly influencing ~500,000 cells<sup>59</sup>) and brief pulses of iES are unlikely to meet these demands, and additionally, transmodal areas themselves are probably poorly placed to directly perturb (or give rise to) experience. Their preferential phylogenetic expansion<sup>60</sup>, complex dendritic arborization<sup>61</sup>, highly variable intrinsic connectivity<sup>17</sup>, high synaptic plasticity<sup>62</sup>, non-specific neuronal tuning<sup>50–57</sup> and abstract functional roles<sup>17,63</sup> all suggest that, instead, they are specialized for the interpretation, manipulation and regulation of more concrete information originating at the base of the cortical hierarchy. Given all of the above considerations, higher elicitation rates in unimodal networks and lower rates in heteromodal and transmodal networks are reasonable, although the specific basis of these inter-network differences remains an open question.

One well-founded concern is that iES effects on transmodal networks could be: (1) more amorphous and therefore harder for patients to describe; or (2) more easily confused with ongoing spontaneous cognition than the relatively simple and concrete perceptual effects elicited in unimodal networks. Both scenarios would result in under-reporting by patients (that is, increased false negatives, or type II errors) and subsequent underestimates of true elicitation rates, and neither possibility should be entirely discounted. However, the first concern is mitigated by the fact that patients are often eloquent and persistent in reporting nuanced and unusual experiences, as demonstrated by many case reports of complex, singular iES effects<sup>21,22,34–36</sup>. Although under-reporting of some subtle effects remains a possibility, such a scenario seems unlikely to explain the very large (greater than fourfold) differences in elicitation rate between networks at the base and apex of the cortical hierarchy. As for the second concern, transmodal networks (particularly the default network) are intimately involved in the generation of the spontaneous mind wandering that occurs during the resting state<sup>64,65</sup>. In principle, then, iES might elicit effects in these networks that are indistinguishable from the ongoing thoughts, imagery and memories generated spontaneously at rest<sup>66</sup>, leading to false negative reports. Again, while this possibility should not be ignored, several factors mitigate the likelihood that it either explains or biases our findings. First, mind wandering is most prevalent during the most minimally demanding and task-free states, and in environments with minimal sensory stimulation<sup>67–69</sup>. Although our patients were given no task during iES, sessions typically involved dozens to hundreds of sequential stimulations each followed by first-person reports, and all undertaken in a busy in-patient hospital setting with multiple researchers present—far-from-ideal conditions for the facilitation of spontaneous thought. Second, although the nature of iES does not permit a precise estimation of the probability of false negative reports (type II errors), our quantitative assessment of false positive reports found that patients were highly resilient to type I errors following sham stimulation. This indicates that, in general, patients discriminate extremely well between background mental activity and

experiences elicited directly by iES. Combined with the demonstrated ability of patients to describe unusual experiences<sup>21,22,34–36</sup> and accurately identify iES-elicited memories<sup>70</sup>, the likelihood seems low that false negatives alone can explain low elicitation rates in transmodal networks.

Despite considerably lower elicitation rates, iES of transmodal regions did sometimes elicit effects (especially in the orbitofrontal cortex and anterior cingulate; Fig. 2a). These findings are perhaps rooted in the variable functional coupling between transmodal and unimodal networks<sup>71</sup>; that is, the specifics of spontaneous network coupling at the precise moment of stimulation could impact whether or not iES perturbs experience—a hypothesis that can be further tested in future work<sup>72</sup>. Importantly, the almost total quiescence in some regions (especially the anterior prefrontal cortex) does not necessarily mean that stimulation there has no consequences. We administered iES in a task-free resting state, but stimulation during demanding executive tasks, for instance, might have measurable effects on performance<sup>73</sup>, if not on subjective experience. Further research exploring iES effects in quiescent regions would be a welcome addition to the ongoing debate on the role of higher-order, transmodal cortical regions in conscious experience<sup>58,74</sup>.

Why was the elicitation rate so low overall? The global rate throughout the brain was ~37%, and even in unimodal networks, iES only elicited effects about half the time. Probably the most plausible and parsimonious explanation is that over the many decades that iES has been employed in neurosurgical settings, stimulation parameters have gradually been optimized for patient safety and clinical utility, not for effect elicitation. Contemporary stimulation falls within an empirically derived safe window specifying upper limits for charge density<sup>32</sup>, and stimulation within these parameters is evidently adequate to elicit motor effects and trigger seizures at epileptic foci (serving the dual clinical aims of identifying tissue that should be spared or resected, respectively). However, the maximum delivered electrical charge might be too low to guarantee that the perturbation of the brain's ongoing neuroelectrical activity is of sufficient magnitude to always result in reportable or observable effects. This supposition is supported by the fact that higher current amplitudes and frequencies tend to result in both a greater number and greater intensity of both subjective and motor effects<sup>22,30,75–77</sup>. These psychological and behavioural findings are consistent with neurophysiological data showing that increasing charge density results in increases in the area of cortical tissue affected by stimulation<sup>30,31</sup>.

Chronically implanted iES neuromodulation devices are increasingly being used to treat the subjective symptoms and network abnormalities of neuropsychiatric diseases<sup>16</sup>. The success of these interventions ultimately depends on a sophisticated understanding of where stimulation should be administered in individual patients' brains to best modulate both subjective experience and network functioning. Here, we have shown that network membership and connectivity profile are powerful predictors of the frequency, category and diversity of effects elicited with iES, even though intrinsic networks are interlaced throughout the brain in non-intuitive ways, traversing and transcending traditional neuroanatomical landmarks and arbitrary anatomical gyral divisions. This finding has potentially important clinical implications, especially given that these relationships hold even at the level of individual neuroanatomy (Fig. 4). Our results offer further evidence in support of the emerging understanding that network membership (not just classic anatomical coordinates or gyral identity) needs to be considered when determining therapeutic targets for iES neuromodulation<sup>8,13,72,78</sup>. In closing, although first-person reports combined with iES have long played a seminal role in the understanding of local functional properties of the human brain<sup>1</sup>, our study goes beyond previous work by revealing relationships between global patterns of brain organization and iES-elicited effects on human behaviour.

## Methods

**Patient characteristics.** Data were drawn from a pool of 119 patients admitted to the Stanford Hospital for iEEG monitoring of medically refractory epilepsy between 2008 and 2018. We considered all patients who underwent iES sessions and also had computed tomography scans and high-resolution T1-weighted MRI scans available for precise reconstruction of electrode locations for inclusion in the present study. We made every effort to include as many patients as possible in order to ensure complete coverage of the cortical mantle; however, many patients could not be included because of: (1) the lack of iES sessions conducted; (2) the lack of high-quality computed tomography scans for the determination of precise electrode locations; (3) the lack of patient-specific anatomical MRI scans for the reconstruction of precise electrode locations in the patient's native brain space; and (4) the lack of electrodes covering the cortical grey matter (for example, in patients implanted solely with depth electrode arrays). Patients were never excluded based on iES elicitation rates, iES effect types or any of our other dependent measures (indeed, these measures were not coded, classified or analysed until after the initial patient pool had been assembled). Patients were only excluded based on the purely practical considerations detailed above. Ultimately our sample comprised 67 patients (28 female (42%); mean age ( $\pm$ s.d.) =  $35.4 \pm 12.7$  years).

It should be noted that most patients who are implanted with intracranial electrodes have been assessed previously with several lines of diagnostic tests and have been deemed to be suffering from focal seizures. These patients most often do not have diffuse brain disease and are implanted because a single seizure focus has been strongly suggested by pre-operative tests (for example, scalp EEG and seizure semiology). As we have discussed at length recently<sup>59</sup>, in patients with focal disease, only the epileptic tissue shows pathological electrophysiological activity (and even this pathological activity is largely time limited<sup>79</sup>), while electrodes outside the epileptic tissue show normal responses to perceptual stimuli during cognitive tasks. Each patient is implanted with a large number of electrodes (100–200), and typically only a minority of electrodes exhibit epileptic activity, while the majority of electrodes show no signs of epileptic discharges.

**Ethics and patient privacy.** All patients provided informed consent in accordance with the Stanford Institutional Review Board for human experiments. Approval for conducting the proposed research was obtained through the Stanford University Institutional Review Board. To ensure confidentiality of the participants' information, all data were de-identified and arbitrary codes were assigned to each patient's data.

**Physical parameters, placement and localization of intracranial electrodes.** Patients were implanted with either subdural grid/strip electrode arrays ( $n = 53$  patients), depth electrodes (stereo-EEG;  $n = 11$  patients) or a mix of both ( $n = 3$  patients), made by Ad-Tech Medical. Subdural electrode arrays are flexible silicon sheets with circular, disc-shaped electrical contacts 2.3 mm in diameter interspersed 10 mm apart. For depth electrodes, each probe consisted of 8–10 electrode contacts spaced 5 mm apart. Contacts were cylindrically shaped (length: 2.4 mm; diameter: 1.3 mm; approximate total surface area: 12 mm<sup>2</sup>). The impedance of electrodes was <1,000  $\Omega$ , and both depth and subdural electrodes had the same hardware impedance. However, the impedance of each contact may have differed depending on the characteristics of the cortical or subcortical tissue it had been implanted over or within. Despite this, our electrical stimulator was designed to adjust the voltage depending on the measured impedance of the electrode and, by doing so, keep the delivered current constant. These co-called constant-current electrical stimulation devices ensured that the delivered current was the intended amount regardless of any minor fluctuations of the local impedance.

Across all patients, we ultimately gathered data from 1,476 subdural grid/strip electrodes and 61 depth electrodes. The placement of all electrodes was determined strictly according to clinical criteria. To precisely determine electrode locations for each patient, electrodes localized in a postoperative computed tomography scan were linearly projected onto the cortical surface reconstructed from a pre-operative T1-weighted MRI scan using the iELVis toolbox<sup>23</sup>. First, the T1 scan was processed and automatically segmented using FreeSurfer version 6.0 (using the recon-all command) to reconstruct the pial, leptomeningeal and inflated cortical surfaces<sup>80,81</sup>. A post-implant computed tomography image was spatially registered to the space of the higher-resolution T1 scan using a rigid transformation (six degrees of freedom; affine mapping). Using BioImage Suite<sup>82</sup>, we manually labelled the electrode locations on the T1-registered computed tomography image. The electrode locations were then projected onto the leptomeningeal surface to correct for possible post-implant brain shift, using an iterative optimization algorithm<sup>83</sup>. The resulting individual surface and volume coordinates were used for visualization. To pool all of the results, electrodes in patient-specific space were normalized to Montreal Neurological Institute (MNI) space and displayed on the fsaverage6 template MNI brain in the FreeSurfer software package<sup>84</sup>.

**Inclusion of depth electrodes.** A limited number of depth electrode contacts were included, to increase the coverage of brain areas where the use of subdural strips and grids is rare (for example, the medial prefrontal cortex). Specifically, depth electrode contacts near either the brain's medial walls or the ventral surface of the

frontal lobe were manually identified and included, to improve the sparse coverage of these transmodal regions and to provide a comprehensive map of the entire cortex. To identify depth electrode contacts near the cortical surfaces, two authors (K.C.R.F. and L.S.) manually delineated the extent of the first gyrus along either the medial or ventral surface for each electrode and for each patient individually (that is, depth electrodes were visualized on coronal brain sections for each patient and only electrode contacts that fell within the grey matter of the gyri along the medial or ventral surface were included in our analyses). Typically, this included only the deepest one or two contacts for each depth electrode; white matter sites were never included in our analysis.

**Excluded brain regions.** Commonly employed intrinsic brain network maps include only the cortical surface<sup>5</sup>; therefore, all subcortical brain regions were excluded using this standard anatomical atlas<sup>5</sup>. Although the hippocampus and insula are considered cortical structures, depth electrode contacts situated in these regions were also not included in the present study, for several reasons. First, transforming deep-depth electrode contacts onto surface (vertex) space is problematic<sup>23</sup>; the error involved in forcing deep-depth electrode contacts into surface space entails a corresponding inaccuracy in assigning these electrodes to a particular intrinsic brain network. Second, the majority of epileptic seizures are known to originate in or near medial temporal lobe structures<sup>85</sup>—a pattern we observed in our pool of patients as well<sup>21</sup>: iES in these areas in our patients typically leads to pathological after-discharges and/or induction of seizures. We therefore opted to exclude electrodes from these deep cortical structures in our study.

**Intracranial electrical stimulation.** Patients underwent iES as part of a routine clinical mapping procedure to determine localization of function and seizure focus<sup>29,59</sup>. In an ideal session, iES was systematically delivered to every electrode contact in a pseudo-random order to which the patient was blind, but time constraints and other clinical considerations (for example, seizure occurrence) sometimes precluded stimulation of every contact in every patient. The specifics of stimulation were at the discretion of the neurologist administering the iES session (J.P.). Typically, bipolar stimulation was delivered using an alternating square wave current applied across two adjacent electrodes at 50 Hz, 2–10 mA current and a pulse width of 200–300  $\mu$ s. If we noticed after-discharges, we reduced the stimulation current immediately. Safe after-discharge limits were never superseded. Further details of stimulation methods and parameters are described extensively in our previous work<sup>30,86</sup>.

Occasional sham stimulations were also delivered to control for demand characteristics, particularly when unusual or intense effects were reported. During sham stimulation, the experimenter behaved exactly as during veridical stimulation, adjusting settings on the stimulator and pressing the same buttons, followed by the same standardized questions about any changes in the patient's experience, the only difference being that no current was actually delivered. Following each iES pulse or sham stimulation, patients were asked standardized, open-ended questions about any experiences evoked (for example, "Did you notice anything?" or "Any change?"), with occasional follow-up questions, as needed, to further clarify the character of effects. Specific iES parameters and elicited effects (or lack thereof) were logged for each stimulation.

**Safety of iES.** The electrical brain stimulation used in this study is routinely employed in clinical practice with an excellent safety profile<sup>19,32</sup>. The amount of electrical charge delivery per pulse was always kept within established safe limits (below 30  $\mu$ C cm<sup>-2</sup> pulse<sup>-1</sup>)<sup>87,88</sup>.

**Controlling for ictal phenomena and other potential confounds.** To preclude the confounding effects of any ictal phenomena, we ensured that none of the patients had an epileptic focus within, or required resection of, the regions included in the present dataset. Some patients had electrode grids placed over the ventral surface of the orbitofrontal cortex; any smell-related effects elicited by stimulation of electrodes along the midline of the ventral surface were excluded from all analyses as potentially confounded by stimulation of the olfactory nerve, as detailed in our previous work<sup>21</sup>.

**Evaluating and classifying the effects of stimulation.** We considered an effect of stimulation valid only if: (1) the tissue stimulated was not later determined to be pathological or resected; (2) stimulation at a given site did not result in seizure(s) or after-discharges; (3) repeated stimulation (one or more repetitions) at the same site in the same patient produced the same or a very similar effect; and (4) sham stimulation at a given site did not result in any false positive reports. Assuming these conditions were met, a patient's report of any change or experience (whether objectively verifiable, as with motor effects, or entirely subjective, as with emotional changes) was considered valid and the stimulating electrode was classified as responsive. Repeated stimulations at sites yielding positive effects were conducted whenever possible, but time and other clinical considerations precluded the replication of every observed effect. Silent electrode sites where iES did not elicit an effect were also generally stimulated multiple times, with increasing current magnitude, to confirm the null effect. As discussed in the text, this ensured that the null effects we observed were not due to inadequate current delivery

(within safe limits); indeed, the mean current at which null effects were observed exceeded the mean current required to elicit an effect for every brain network we investigated. Therefore, far from being the result merely of inadequate current delivery, our null findings in fact persisted even following the administration of considerably greater current magnitude than was typically required to elicit a response (see Tables 1 and 2).

Stimulation of motor and premotor areas in the superior parietal and frontal lobes often resulted in observable motor effects, from small muscle twitches to larger limb movements, in line with extensive previous research<sup>89,90</sup>. Even though the effects for these trials were readily observable, they were coded based not just on observed behaviour but also the patient's first-person report of their experience of motor movement (for specific, verbatim examples, see Fig. 6).

Three raters (K.C.R.F., L.S. and S.B.), who were blind to both the location and network assignment of each electrode, viewed and coded digitized iES reports and video-EEG recordings to confirm the results. As the first aim of the present study was to further investigate our recent observations of apparent silence following iES to transmodal brain regions<sup>21,86</sup>, initially a simple binary coding scheme was employed: (1) responsive (that is, any reportable effect on subjective experience or observable effect on motor output); or (2) silent (that is, null; no discernible effect on body or subjective experience, even with repeated stimulation at high current levels (within safe limits)). Details of the number of responsive versus silent electrodes are given in Table 1 (seven-network parcellation) and Table 2 (17-network parcellation).

As noted above, iES was delivered using bipolar stimulation (that is, current was delivered to brain tissue by creating a voltage difference across two adjacent electrode contacts). All effects (and null results) were therefore observed across pairs of electrodes; for purposes of visualization and statistical analysis of the data, each electrode was coded individually as either responsive or silent (Fig. 1). Occasionally, a given electrode was paired with more than one other partner electrode during subsequent stimulations. Typically, the same effect (or lack thereof) was observed, but in rare instances, a given electrode might show differential effects with different electrode pairings (for example, responsive with one pairing and null with another). In such cases, a conservative approach was taken (as per our Methods above): the null hypothesis was always assumed, and an effect had to be reproducible upon repeated stimulation at the same site to be counted as valid and included in subsequent analyses. Therefore, given a set of three adjacent electrodes (*a*, *b*, *c*), if pairing *b*–*c* resulted in an effect, but pairing *a*–*b* did not, electrodes *a* and *b* would be coded as silent and only electrode *c* would be coded as responsive. The conservative assumption being employed is that brain tissue surrounding electrode *c* is the primary driver of the reported effect following stimulation of the *b*–*c* electrode pair, since stimulation of the *a*–*b* pair yields no effect.

For each electrode coded as responsive, two raters (K.C.R.F. and L.S.) then classified the specific qualities of the effects using broad, data-driven categories, as in our previous work<sup>21</sup>. Ultimately, eight categories were employed: (1) somatomotor effects, including somatosensations and any observable motor effects, such as muscle twitches or limb movements; (2) visual effects, from simple phosphenes to more complex perturbations of visual perception such as distortion of faces; (3) olfactory effects, described in detail in our recent work<sup>21</sup>; (4) vestibular effects, such as feelings of rotation, flotation and acceleration; (5) emotional effects of either positive or negative valence, also described in more detail in our recent research<sup>21</sup>; (6) language effects, including arrest or alteration (for example, slurring) of speech; (7) memory recall; and (8) physiological and interoceptive effects, such as perceived changes in body temperature or heart rate. Classified results were then pooled to yield an estimate of the prevalence of each effect type for each brain network (Extended Data Figs. 4 and 5). To clarify further, no type of effect was excluded a priori: our categorizations were entirely data driven and included all valid effects elicited by electrodes in healthy brain tissue. Notably, we never observed some striking iES effects reported by other researchers, such as out-of-body experiences<sup>35</sup> or elicitation of the intention to move<sup>36</sup>. Conversely, we observed rare but replicable effects (such as the will to persevere<sup>34</sup>) not yet reported by other researchers in nearly a century of iES studies. There are many potential reasons for such discrepancies; however, we suspect that the major reason is simply the relatively small number of researchers and studies exploring the effects of iES. In any event, we wish to reiterate that no effect type was excluded, but rather that even in our comparatively large sample of iES patients, not every possible type of effect was found to be elicited.

**Assigning electrodes to intrinsic brain networks.** We aggregated information from 1,537 unique electrode sites at which iES had been applied in 67 patients (Fig. 1). Electrodes were assigned to a given intrinsic network using an algorithm implemented in the iELVis software package<sup>23</sup>. Briefly, an electrode's vertex location in cortical surface space was compared with standardized maps of intrinsic brain network parcellations based on resting-state fMRI data from 1,000 healthy participants<sup>5</sup>, and the electrode was assigned to the nearest network<sup>23</sup>. Network assignments were made in individual patients' neuroanatomical space, after which data were collated in standard space for visualization purposes (Fig. 1). For the carefully selected (see above) depth electrode contacts near the medial cortical surfaces, the algorithm was modified slightly to assign the volume-based

depth electrode coordinates to the nearest surface vertex coordinate, and network assignment was then based on this vertex coordinate. The most commonly used intrinsic brain network atlases include seven-network and 17-network parcellations of the cerebral cortex<sup>5</sup>; we employed both parcellation schemes. Details of the number of electrodes assigned to each network are given in Table 1 (seven-network parcellation) and Table 2 (17-network parcellation).

**Estimating elicitation rate for brain networks.** We first pooled data on responsive and silent electrodes from all patients for every given network (Fig. 1). We then divided the number of responsive electrodes by the total number of electrodes in each network to estimate network-specific elicitation rates for both seven-network (Table 1) and 17-network (Table 2) parcellations of the cerebral cortex. All details of the data are available in Tables 1 and 2.

**Reliability of elicitation rate.** To ensure that our estimates of elicitation rate for each network were stable and replicable, we conducted a series of reliability analyses by splitting our large dataset (1,537 unique electrodes) in three different, independent ways. We estimated network-specific elicitation rates using these subsamples and compared them with the elicitation rates based on the full dataset (which included all electrodes). First, we calculated elicitation rates separately for electrodes on the medial wall versus the lateral surface (including ventral surfaces) of the cerebral cortex. Second, we randomly divided our pool of 67 patients into discovery ( $N = 33$  patients;  $n = 777$  electrodes) and replication ( $N = 34$  patients;  $n = 760$  electrodes) samples and calculated global (medial + lateral) network elicitation rates for each group. Finally, we used an algorithm to randomly select half of our electrodes and calculate elicitation rates for each network based on this subset of all electrodes; this process was repeated over 100 iterations, and average elicitation rates for each network from all iterations were employed.

In all cases, the reliability sample estimates correlated extremely well with the elicitation rates derived from our full dataset, for both seven-network (Supplementary Table 1) and 17-network (Supplementary Table 2) parcellations of the cerebral cortex. Elicitation rates based on our reliability samples also closely mirrored our central finding of the relationship between elicitation rate and principal gradient hierarchy values (Extended Data Figs. 2 and 3).

**Principal gradient hierarchy values.** The principal gradient hierarchy values were derived from a nonlinear embedding of functional connectivity patterns. The principal gradient represents the first latent dimension of this embedding space, which captures the largest variance in functional connectivity patterns, and reflects a spatial gradient of increasingly abstract and integrated processing from primary sensory/motor cortices to transmodal regions. The specific methodology employed to derive the principal gradient is described in detail in the original empirical report<sup>17</sup>. For the present study, vertex-level principal gradient hierarchy values were averaged for standardized seven-network and 17-network parcellations of the cerebral cortex<sup>5</sup>, and these averaged, network-level principal gradient values were correlated with our network-level elicitation rates. Vertex-level (as opposed to network-averaged) principal gradient values were also employed in additional analyses (see next section).

**Mixed-effects binary logistic regression.** Our central analyses showed a strong relationship between mean network elicitation rates and mean network principal gradient values. However, such an approach restricts the full range of principal gradient values, and also relies on somewhat arbitrary intrinsic network boundaries (in that multiple intrinsic network parcellations are equally valid; see Fig. 6 in ref. <sup>5</sup>). Therefore, to further confirm our findings independent of network parcellations, and across the gradient's full range, we extracted principal gradient values at each vertex in cortical surface space where iES had been administered. Because of inaccuracies in assigning specific vertex (and hence principal gradient) values to depth electrodes, these electrodes were excluded from this analysis. Several more electrodes could also not be assigned specific principal gradient values due to errors in alignment of the two datasets. Together, these excluded electrodes ( $n = 103$ ) represented a very small proportion of the overall dataset, and the final logistic regression included 93.3% of our original sample ( $n = 1,434$  electrode sites). We implemented binary logistic regression to explore the association between principal gradient value (fixed effect) and our binary coding of electrode sites (silent/responsive) as the dependent variable. Further details are provided in Supplementary Tables 3 and 4.

**Estimating the prevalence and heterogeneity of different effect types across networks and their relationship with the principal gradient.** As described above, we classified the effects at all responsive electrodes into one of eight broad, data-driven categories. The prevalence of each effect type was tabulated for all networks for both the seven-network (Extended Data Fig. 4) and 17-network (Extended Data Fig. 5) parcellations of the cerebral cortex. To assess the relationship between network membership and the categorized type of effect, we estimated the  $\lambda$  coefficient—a measure of association appropriate for nominal (that is, categorical) variables. To provide a simple measure of the diversity of effect types elicited in each network, we summed the number of categories of different effect types elicited in each network (Fig. 5b,d). This diversity measure was related

to the principal gradient value using a Pearson correlation to assess whether a network's position in the hierarchy was related to the diversity of effects elicited within a given network. Partial correlations were also conducted controlling for the total number of responsive electrodes in each network, to account for the fact that transmodal networks higher in the hierarchy tended to exhibit far fewer responsive electrodes overall.

**Mean current elicitation and quiescence thresholds.** The factors contributing to the excitability of cortical tissue following iES remain poorly understood<sup>1,30</sup>. To explore whether differential elicitation rates might be explained by variance in tissue excitability across networks, the amount of current delivered (mA) was logged for each instance of stimulation. For each responsive electrode, we identified the minimum current required to elicit an effect. We then calculated a mean elicitation threshold for each network by averaging these minimum required currents for all electrodes within a given network. The mean minimum elicitation thresholds for each network are presented in Table 1 (seven-network parcellation) and Table 2 (17-network parcellation).

Furthermore, to ensure that the high rate of null effects in transmodal networks was not due simply to inadequate current delivery, the maximum delivered current yielding no effect for every silent electrode was also tabulated, then averaged for each network. For all networks, this mean maximum quiescence threshold exceeded the mean current required to elicit an effect in the same network (that is, null effects were still observed despite higher mean current delivery than at electrodes where iES elicited effects in the same network (see also main text)). The mean maximum quiescence thresholds for each network are presented in Table 1 (seven-network parcellation) and Table 2 (17-network parcellation).

**Intracortical myelin content.** Intracortical myelin content (sometimes referred to as myelin density) is known to vary across intrinsic brain networks, with heavier myelination in unimodal networks and lighter myelination in transmodal networks<sup>4,33</sup>. To explore whether regional differences in myelination might be associated with differential elicitation rates across networks, we accessed publicly available data from the Human Connectome Project<sup>18</sup> that estimated regional white matter density throughout the brain using the ratio of T1-weighted to T2-weighted MRI signal. We averaged these data for each network, using both seven-network and 17-network parcellations, to obtain mean myelin density measures for each network, and then compared these with elicitation rates for each network as determined in our iES sessions.

**Statistical analyses.** Most statistical tests were conducted using SPSS 20 (IBM), with a significance threshold of  $\alpha = 0.05$  (two tailed). For null findings, Jeffreys–Zellner–Siow Bayes factors<sup>91</sup> were used to estimate the likelihood of the null versus alternative hypotheses; these analyses were implemented in SPSS 26 (IBM).

**Reporting Summary.** Further information on research design is available in the Nature Research Reporting Summary linked to this article.

## Data availability

The data that support the findings of this study are available from the corresponding authors upon request.

## Code availability

Custom code that supports the findings of this study is available from the corresponding authors upon request.

Received: 21 June 2019; Accepted: 4 June 2020;

Published online: 06 July 2020

## References

- Borchers, S., Himmelbach, M., Logothetis, N. & Karnath, H.-O. Direct electrical stimulation of human cortex—the gold standard for mapping brain functions? *Nat. Rev. Neurosci.* **13**, 63–70 (2012).
- Penfield, W. & Perot, P. The brain's record of auditory and visual experience: a final summary and discussion. *Brain* **86**, 595–696 (1963).
- Penfield, W. & Rasmussen, T. *The Cerebral cortex of Man: a Clinical Study of Localization of Function* (Macmillan, 1950).
- Huntenburg, J. M., Bazin, P.-L. & Margulies, D. S. Large-scale gradients in human cortical organization. *Trends Cogn. Sci.* **22**, 21–31 (2018).
- Yeo, B. T. T. et al. The organization of the human cerebral cortex estimated by intrinsic functional connectivity. *J. Neurophysiol.* **106**, 1125–1165 (2011).
- Power, J. D. et al. Functional network organization of the human brain. *Neuron* **72**, 665–678 (2011).
- Alhourani, A. et al. Network effects of deep brain stimulation. *J. Neurophysiol.* **114**, 2105–2117 (2015).
- Khambhati, A. N. et al. Functional control of electrophysiological network architecture using direct neurostimulation in humans. *Netw. Neurosci.* **3**, 848–877 (2019).
- Keller, C. J. et al. Induction and quantification of excitability changes in human cortical networks. *J. Neurosci.* **38**, 5384–5398 (2018).
- Shine, J. M. et al. Distinct patterns of temporal and directional connectivity among intrinsic networks in the human brain. *J. Neurosci.* **37**, 9667–9674 (2017).
- Solomon, E. et al. Medial temporal lobe functional connectivity predicts stimulation-induced theta power. *Nat. Commun.* **9**, 4437 (2018).
- Keller, C. J. et al. Intrinsic functional architecture predicts electrically evoked responses in the human brain. *Proc. Natl Acad. Sci. USA* **108**, 10308–10313 (2011).
- Betzel, R. F. et al. Structural, geometric and genetic factors predict interregional brain connectivity patterns probed by electrocorticography. *Nat. Biomed. Eng.* **3**, 902–916 (2019).
- Mayberg, H. S., Riva-Posse, P. & Crowell, A. L. Deep brain stimulation for depression: keeping an eye on a moving target. *JAMA Psychiatry* **73**, 439–440 (2016).
- Morishita, T., Fayad, S. M., Higuchi, M.-A., Nestor, K. A. & Foote, K. D. Deep brain stimulation for treatment-resistant depression: systematic review of clinical outcomes. *Neurotherapeutics* **11**, 475–484 (2014).
- Famm, K., Litt, B., Tracey, K. J., Boyden, E. S. & Slaoui, M. A jump-start for electroceuticals. *Nature* **496**, 159–161 (2013).
- Margulies, D. S. et al. Situating the default-mode network along a principal gradient of macroscale cortical organization. *Proc. Natl Acad. Sci. USA* **113**, 12574–12579 (2016).
- Glasser, M. F. & Van Essen, D. C. Mapping human cortical areas in vivo based on myelin content as revealed by T1- and T2-weighted MRI. *J. Neurosci.* **31**, 11597–11616 (2011).
- Goldstein, H. E. et al. Risk of seizures induced by intracranial research stimulation: analysis of 770 stimulation sessions. *J. Neural Eng.* **16**, 066039 (2019).
- Awad, I. A., Rosenfeld, J., Ahl, J., Hahn, J. F. & Lüders, H. Intractable epilepsy and structural lesions of the brain: mapping, resection strategies, and seizure outcome. *Epilepsia* **32**, 179–186 (1991).
- Fox, K. C. R. et al. Changes in subjective experience elicited by direct stimulation of the human orbitofrontal cortex. *Neurology* **91**, e1519–e1527 (2018).
- Yih, J., Beam, D. E., Fox, K. C. R. & Parvizi, J. Intensity of affective experience is modulated by magnitude of electrical stimulation in human orbitofrontal, cingulate, and insular cortices. *Soc. Cogn. Affect. Neurosci.* **14**, 339–351 (2019).
- Groppe, D. M. et al. iELVis: an open source MATLAB toolbox for localizing and visualizing human intracranial electrode data. *J. Neurosci. Methods* **281**, 40–48 (2017).
- Rangarajan, V. et al. Electrical stimulation of the left and right human fusiform gyrus causes different effects in conscious face perception. *J. Neurosci.* **34**, 12828–12836 (2014).
- Goldberg, E. Gradiational approach to neocortical functional organization. *J. Clin. Exp. Neuropsychol.* **11**, 489–517 (1989).
- Mesulam, M.-M. From sensation to cognition. *Brain* **121**, 1013–1052 (1998).
- Damasio, A. R. & Damasio, H. in *Large-Scale Neuronal Theories of the Brain* (eds Koch, C. & Davis, J. L.) 61–74 (MIT Press, 1994).
- Jones, E. & Powell, T. An anatomical study of converging sensory pathways within the cerebral cortex of the monkey. *Brain* **93**, 793–820 (1970).
- Selimbeyoglu, A. & Parvizi, J. Electrical stimulation of the human brain: perceptual and behavioral phenomena reported in the old and new literature. *Front. Hum. Neurosci.* **4**, 46 (2010).
- Winawer, J. & Parvizi, J. Linking electrical stimulation of human primary visual cortex, size of affected cortical area, neuronal responses, and subjective experience. *Neuron* **92**, 1213–1219 (2016).
- Mohan, U. R. et al. The effects of direct brain stimulation in humans depend on frequency, amplitude, and white-matter proximity. *Brain Stim.* **13**, 1183–1195 (2020).
- Gordon, B. et al. Parameters for direct cortical electrical stimulation in the human: histopathologic confirmation. *Electroencephalogr. Clin. Neurophysiol.* **75**, 371–377 (1990).
- Huntenburg, J. M. et al. A systematic relationship between functional connectivity and intracortical myelin in the human cerebral cortex. *Cereb. Cortex* **27**, 981–997 (2017).
- Parvizi, J., Rangarajan, V., Shirer, W. R., Desai, N. & Greicius, M. D. The will to persevere induced by electrical stimulation of the human cingulate gyrus. *Neuron* **80**, 1359–1367 (2013).
- Blanke, O., Ortigue, S., Landis, T. & Seeck, M. Stimulating illusory own-body perceptions. *Nature* **419**, 269–270 (2002).
- Desmurget, M. et al. Movement intention after parietal cortex stimulation in humans. *Science* **324**, 811–813 (2009).
- Rangarajan, V. & Parvizi, J. Functional asymmetry between the left and right human fusiform gyrus explored through electrical brain stimulation. *Neuropsychologia* **83**, 29–36 (2016).

38. Toga, A. W. & Thompson, P. M. Mapping brain asymmetry. *Nat. Rev. Neurosci.* **4**, 37–48 (2003).
39. Histed, M. H., Ni, A. M. & Maunsell, J. H. Insights into cortical mechanisms of behavior from microstimulation experiments. *Prog. Neurobiol.* **103**, 115–130 (2013).
40. Desmurget, M., Song, Z., Mottolose, C. & Sirigu, A. Re-establishing the merits of electrical brain stimulation. *Trends Cogn. Sci.* **17**, 442–449 (2013).
41. Azarfar, A., Calcini, N., Huang, C., Zeldenrust, F. & Celikel, T. Neural coding: a single neuron's perspective. *Neurosci. Biobehav. Rev.* **94**, 238–247 (2018).
42. Horton, J. C. & Adams, D. L. The cortical column: a structure without a function. *Phil. Trans. R. Soc. B Biol. Sci.* **360**, 837–862 (2005).
43. Patel, G. H., Kaplan, D. M. & Snyder, L. H. Topographic organization in the brain: searching for general principles. *Trends Cogn. Sci.* **18**, 351–363 (2014).
44. Grill-Spector, K. & Malach, R. The human visual cortex. *Annu. Rev. Neurosci.* **27**, 649–677 (2004).
45. Bendor, D. & Wang, X. The neuronal representation of pitch in primate auditory cortex. *Nature* **436**, 1161–1165 (2005).
46. Anzai, A., Peng, X. & Van Essen, D. C. Neurons in monkey visual area V2 encode combinations of orientations. *Nat. Neurosci.* **10**, 1313–1321 (2007).
47. Hegd , J. & Van Essen, D. C. Selectivity for complex shapes in primate visual area V2. *J. Neurosci.* **20**, RC61–RC61 (2000).
48. Dobbins, A., Zucker, S. W. & Cynader, M. S. Endstopped neurons in the visual cortex as a substrate for calculating curvature. *Nature* **329**, 438–441 (1987).
49. Andermann, M. L. & Moore, C. I. A somatotopic map of vibrissa motion direction within a barrel column. *Nat. Neurosci.* **9**, 543–551 (2006).
50. Mante, V., Sussillo, D., Shenoy, K. V. & Newsome, W. T. Context-dependent computation by recurrent dynamics in prefrontal cortex. *Nature* **503**, 78–84 (2013).
51. Rigotti, M. et al. The importance of mixed selectivity in complex cognitive tasks. *Nature* **497**, 585–590 (2013).
52. Ekstrom, A. D. et al. Cellular networks underlying human spatial navigation. *Nature* **425**, 184–188 (2003).
53. Rolls, E. T. & Baylis, L. L. Gustatory, olfactory, and visual convergence within the primate orbitofrontal cortex. *J. Neurosci.* **14**, 5437–5452 (1994).
54. Schultz, W., Tremblay, L. & Hollerman, J. R. Reward processing in primate orbitofrontal cortex and basal ganglia. *Cereb. Cortex* **10**, 272–283 (2000).
55. Quiroga, R. Q., Reddy, L., Kreiman, G., Koch, C. & Fried, I. Invariant visual representation by single neurons in the human brain. *Nature* **435**, 1102–1107 (2005).
56. Gelbard-Sagiv, H., Mukamel, R., Harel, M., Malach, R. & Fried, I. Internally generated reactivation of single neurons in human hippocampus during free recall. *Science* **322**, 96–101 (2008).
57. McCoy, A. N. & Platt, M. L. Risk-sensitive neurons in macaque posterior cingulate cortex. *Nat. Neurosci.* **8**, 1220–1227 (2005).
58. Odegaard, B., Knight, R. T. & Lau, H. Should a few null findings falsify prefrontal theories of conscious perception? *J. Neurosci.* **37**, 9593–9602 (2017).
59. Parvizi, J. & Kastner, S. Promises and limitations of human intracranial electroencephalography. *Nat. Neurosci.* **21**, 474–483 (2018).
60. Hill, J. et al. Similar patterns of cortical expansion during human development and evolution. *Proc. Natl Acad. Sci. USA* **107**, 13135–13140 (2010).
61. Jacobs, B. et al. Regional dendritic and spine variation in human cerebral cortex: a quantitative golgi study. *Cereb. Cortex* **11**, 558–571 (2001).
62. Garc a-Cabezas, M. A., Joyce, M. K. P., John, Y. J., Zikopoulos, B. & Barbas, H. Mirror trends of plasticity and stability indicators in primate prefrontal cortex. *Eur. J. Neurosci.* **46**, 2392–2405 (2017).
63. Fox, K. C. R., Foster, B. L., Kucyi, A., Daitch, A. L. & Parvizi, J. Intracranial electrophysiology of the human default network. *Trends Cogn. Sci.* **22**, 307–324 (2018).
64. Fox, K. C. R., Spreng, R. N., Ellamil, M., Andrews-Hanna, J. R. & Christoff, K. The wandering brain: meta-analysis of functional neuroimaging studies of mind-wandering and related spontaneous thought processes. *NeuroImage* **111**, 611–621 (2015).
65. Christoff, K., Irving, Z. C., Fox, K. C. R., Spreng, R. N. & Andrews-Hanna, J. R. Mind-wandering as spontaneous thought: a dynamic framework. *Nat. Rev. Neurosci.* **17**, 718–731 (2016).
66. Fox, K. C. R., Andrews-Hanna, J. R. & Christoff, K. The neurobiology of self-generated thought from cells to systems: integrating evidence from lesion studies, human intracranial electrophysiology, neurochemistry, and neuroendocrinology. *Neuroscience* **335**, 134–150 (2016).
67. Antrobus, J. S., Singer, J. L. & Greenberg, S. Studies in the stream of consciousness: experimental enhancement and suppression of spontaneous cognitive processes. *Percept. Mot. Skills* **23**, 399–417 (1966).
68. Mason, M. F. et al. Wandering minds: the default network and stimulus-independent thought. *Science* **315**, 393–395 (2007).
69. Lilly, J. C. Mental effects of reduction of ordinary levels of physical stimuli on intact, healthy persons. *Psychiatric Res. Rep.* **5**, 1–9 (1956).
70. Curot, J. et al. Memory scrutinized through electrical brain stimulation: a review of 80 years of experiential phenomena. *Neurosci. Biobehav. Rev.* **78**, 161–177 (2017).
71. Cole, M. W. et al. Multi-task connectivity reveals flexible hubs for adaptive task control. *Nat. Neurosci.* **16**, 1348–1355 (2013).
72. Ezzzyat, Y. et al. Direct brain stimulation modulates encoding states and memory performance in humans. *Curr. Biol.* **27**, 1251–1258 (2017).
73. Ezzzyat, Y. et al. Closed-loop stimulation of temporal cortex rescues functional networks and improves memory. *Nat. Commun.* **9**, 365 (2018).
74. Boly, M. et al. Are the neural correlates of consciousness in the front or in the back of the cerebral cortex? Clinical and neuroimaging evidence. *J. Neurosci.* **37**, 9603–9613 (2017).
75. Fried, I., Wilson, C. L., MacDonald, K. A. & Behnke, E. J. Electric current stimulates laughter. *Nature* **391**, 650 (1998).
76. Inman, C. S. et al. Human amygdala stimulation effects on emotion physiology and emotional experience. *Neuropsychologia* <https://doi.org/10.1016/j.neuropsychologia.2018.03.019> (2018).
77. Bosking, W. H. et al. Saturation in phosphene size with increasing current levels delivered to human visual cortex. *J. Neurosci.* **37**, 7188–7197 (2017).
78. McIntyre, C. C. & Hahn, P. J. Network perspectives on the mechanisms of deep brain stimulation. *Neurobiol. Dis.* **38**, 329–337 (2010).
79. Liu, S. & Parvizi, J. Cognitive refractory state caused by spontaneous epileptic high frequency oscillations in the human brain. *Sci. Transl. Med.* **11**, eaax7830 (2019).
80. Fischl, B., Sereno, M. I. & Dale, A. M. Cortical surface-based analysis: II: inflation, flattening, and a surface-based coordinate system. *NeuroImage* **9**, 195–207 (1999).
81. Fischl, B., Sereno, M. I., Tootell, R. B. & Dale, A. M. High-resolution intersubject averaging and a coordinate system for the cortical surface. *Hum. Brain Mapp.* **8**, 272–284 (1999).
82. Papademetris, X. et al. BioImage Suite: an integrated medical image analysis suite: an update. *Insight J.* **2006**, 209 (2006).
83. Dykstra, A. R. et al. Individualized localization and cortical surface-based registration of intracranial electrodes. *NeuroImage* **59**, 3563–3570 (2012).
84. Fischl, B. FreeSurfer. *NeuroImage* **62**, 774–781 (2012).
85. Semah, F. et al. Is the underlying cause of epilepsy a major prognostic factor for recurrence? *Neurology* **51**, 1256–1262 (1998).
86. Foster, B. L. & Parvizi, J. Direct cortical stimulation of human posteromedial cortex. *Neurology* **88**, 685–691 (2017).
87. Agnew, W. F., Yuen, T. G. & McCreery, D. B. Morphologic changes after prolonged electrical stimulation of the cat's cortex at defined charge densities. *Exp. Neurol.* **79**, 397–411 (1983).
88. Babb, T. L. & Kupfer, W. Phagocytic and metabolic reactions to intracerebral electrical stimulation of rat brain. *Exp. Neurol.* **86**, 183–197 (1984).
89. Penfield, W. & Boldrey, E. Somatic motor and sensory representation in the cerebral cortex of man as studied by electrical stimulation. *Brain* **60**, 389–443 (1937).
90. Fried, I. et al. Functional organization of human supplementary motor cortex studied by electrical stimulation. *J. Neurosci.* **11**, 3656–3666 (1991).
91. Jarosz, A. F. & Wiley, J. What are the odds? A practical guide to computing and reporting Bayes factors. *J. Problem Solving* **7**, 2 (2014).
92. Parvizi, J. et al. Electrical stimulation of human fusiform face-selective regions distorts face perception. *J. Neurosci.* **32**, 14915–14920 (2012).

## Acknowledgements

The authors are grateful to the many patients who participated, without whom this research would have been impossible, as well as numerous funding agencies for generous support. K.C.R.F. was supported by a Postdoctoral Fellowship from the Natural Sciences and Engineering Research Council (NSERC) of Canada, and is currently supported by a Medical Scholars Research Fellowship from the Stanford University School of Medicine. L.S. is supported by the China Scholarship Council (201708110057) and National Natural Science Foundation of China (81701268). B.L.F. is supported by the National Institutes of Health (R00MH103479). A.K. was supported by a Banting Postdoctoral Fellowship from the Canadian Institutes of Health Research (CIHR). J.P. is supported by the National Institutes of Health (1P50MH109429). The funders had no role in study design, data collection and analysis, decision to publish or preparation of the manuscript.

## Author contributions

K.C.R.F., O.R. and J.P. conceived of the study. K.C.R.F., L.S., D.S.M., A.K. and J.P. designed the study. K.C.R.F. and J.P. collected the data. K.C.R.F., L.S., S.B., O.R., B.L.F., S.S., D.S.M. and A.K. analysed the data. K.C.R.F., L.S., S.B. and O.R. created the figures. K.C.R.F. and J.P. wrote the initial draft of the manuscript. All authors participated in writing the final draft.

## Competing interests

The authors declare no competing interests.

**Additional information**

**Extended data** is available for this paper at <https://doi.org/10.1038/s41562-020-0910-1>.

**Supplementary information** is available for this paper at <https://doi.org/10.1038/s41562-020-0910-1>.

**Correspondence and requests for materials** should be addressed to K.C.R.F. or J.P.

**Peer review information** Primary Handling Editor: Marike Schiffer.

**Reprints and permissions information** is available at [www.nature.com/reprints](http://www.nature.com/reprints).

**Publisher's note** Springer Nature remains neutral with regard to jurisdictional claims in published maps and institutional affiliations.

© The Author(s), under exclusive licence to Springer Nature Limited 2020

Network	Left hemisphere	Right hemisphere	Mean difference (t)	p-value
Somatomotor	48.9%	78.6%	4.104*	<.001
Visual	62.0%	41.1%	-2.861*	.005
Dorsal Attention	37.7%	50.0%	0.730	.468
Saliency	41.0%	60.2%	2.801*	.006
Frontoparietal	29.8%	39.5%	1.127	.261
Limbic	23.3%	25.8%	0.378	.706
Default	19.0%	25.2%	1.413	.158
Totals	34.6%	43.4%	3.279*	.001

**Extended Data Fig. 1 | Hemispheric asymmetries in elicitation rate.** For post-hoc individual network comparisons, statistical significance was set at  $p < .007$  ( $\alpha = .05$  Bonferroni-corrected for seven multiple comparisons).

	7-Network Parcellation Elicitation Rates					
	Full dataset	Medial surface	Lateral surface	Discovery sample	Replication sample	Random half of electrodes
Principal Gradient Hierarchy Value	$r = .96$ [.75, .99]	$r = .70$ [-.11, .95]	$r = .86$ [.30, .98]	$r = .84$ [.24, .98]	$r = .84$ [.22, .98]	$r = .93$ [.59, .99]

**Extended Data Fig. 2 | Reliability analyses for 7-network elicitation rates.** Seven-network parcellation: correlations between elicitation rate and principal gradient value across all reliability samples (Pearson's  $r$ , [95% CIs]).

	17-Network Parcellation Elicitation Rates					
	Full dataset	Medial surface	Lateral surface	Discovery sample	Replication sample	Random half of electrodes
Principal Gradient Hierarchy Value	$r = .82$ [.56, .93]	$r = .33$ [-.18, .70]	$r = .83$ [.58, .94]	$r = .72$ [.37, .89]	$r = .76$ [.44, .91]	$r = .83$ [.58, .94]

**Extended Data Fig. 3 | Reliability analyses for 17-network elicitation rates.** 17-network parcellation: correlations between elicitation rate and principal gradient value across all reliability samples (Pearson's  $r$ , [95% CIs]).

Network	Effect Type							
	Somatomotor	Visual	Olfactory	Vestibular	Emotion	Language	Memory	Physiological
<b>Somatomotor</b>	142 (89.3%)	1 (0.6%)	-	1 (0.6%)	1 (0.6%)	14 (8.8%)	-	-
<b>Visual</b>	9 (9.6%)	82 (87.2%)	-	-	-	3 (3.2%)	-	-
<b>Dorsal Attention</b>	7 (25.0%)	13 (46.4%)	-	3 (10.7%)	-	5 (17.9%)	-	-
<b>Salience</b>	71 (68.3%)	9 (8.7%)	-	-	2 (1.9%)	20 (19.2%)	2 (1.9%)	-
<b>Frontoparietal</b>	31 (57.4%)	9 (16.7%)	1 (1.8%)	-	2 (3.7%)	11 (20.4%)	-	-
<b>Limbic</b>	20 (42.6%)	12 (25.5%)	8 (17.0%)	1 (2.1%)	1 (2.1%)	-	4 (8.5%)	1 (2.1%)
<b>Default</b>	40 (46.0%)	17 (19.5%)	3 (3.4%)	4 (4.6%)	5 (5.7%)	16 (18.4%)	-	2 (2.3%)
<b>Totals</b>	320	143	12	9	11	69	6	3

**Extended Data Fig. 4 | Effect categories elicited in the 7-network parcellation.** Frequency of effect types within each network.

Network	Effect Type							
	Somatomotor	Visual	Olfactory	Vestibular	Emotion	Language	Memory	Physiological
01	3 (8.6%)	31 (88.6%)	-	-	-	1 (2.9%)	-	-
02	6 (13.6%)	37 (84.1%)	-	-	-	1 (2.3%)	-	-
03	102 (99.0%)	-	-	1 (1.0%)	-	-	-	-
04	30 (71.4%)	1 (2.4%)	-	-	-	11 (26.2%)	-	-
05	-	16 (76.2%)	-	2 (9.5%)	-	3 (14.3%)	-	-
06	11 (68.8%)	2 (12.5%)	-	1 (6.3%)	-	2 (12.5%)	-	-
07	63 (74.1%)	2 (2.4%)	-	-	2 (2.4%)	17 (19.8%)	1 (1.2%)	-
08	20 (54.1%)	8 (21.6%)	-	-	3 (8.1%)	5 (13.5%)	1 (2.7%)	-
09	15 (62.5%)	8 (33.3%)	-	-	1 (4.2%)	-	-	-
10	5 (20.8%)	3 (12.5%)	9 (37.5%)	2 (8.3%)	-	-	4 (16.7%)	1 (4.2%)
11	10 (47.6%)	8 (38.1%)	-	-	1 (4.8%)	2 (9.5%)	-	-
12	7 (30.4%)	6 (26.1%)	-	-	1 (4.3%)	9 (39.1%)	-	-
13	11 (78.6%)	-	-	1 (7.1%)	-	2 (14.3%)	-	-
14	5 (55.6%)	1 (11.1%)	-	-	-	3 (33.3%)	-	-
15	-	10 (83.3%)	2 (16.7%)	-	-	-	-	-
16	21 (58.3%)	8 (22.2%)	-	1 (2.8%)	3 (8.3%)	1 (2.8%)	-	2 (5.6%)
17	11 (40.7%)	2 (7.4%)	1 (3.7%)	1 (3.7%)	-	12 (44.4%)	-	-
<b>Totals</b>	320	143	12	9	11	69	6	3

Extended Data Fig. 5 | Effect categories elicited in the 17-network parcellation. Frequency of effect types within each network.

## Reporting Summary

Nature Research wishes to improve the reproducibility of the work that we publish. This form provides structure for consistency and transparency in reporting. For further information on Nature Research policies, see [Authors & Referees](#) and the [Editorial Policy Checklist](#).

### Statistics

For all statistical analyses, confirm that the following items are present in the figure legend, table legend, main text, or Methods section.

n/a Confirmed

- The exact sample size ( $n$ ) for each experimental group/condition, given as a discrete number and unit of measurement
- A statement on whether measurements were taken from distinct samples or whether the same sample was measured repeatedly
- The statistical test(s) used AND whether they are one- or two-sided  
*Only common tests should be described solely by name; describe more complex techniques in the Methods section.*
- A description of all covariates tested
- A description of any assumptions or corrections, such as tests of normality and adjustment for multiple comparisons
- A full description of the statistical parameters including central tendency (e.g. means) or other basic estimates (e.g. regression coefficient) AND variation (e.g. standard deviation) or associated estimates of uncertainty (e.g. confidence intervals)
- For null hypothesis testing, the test statistic (e.g.  $F$ ,  $t$ ,  $r$ ) with confidence intervals, effect sizes, degrees of freedom and  $P$  value noted  
*Give  $P$  values as exact values whenever suitable.*
- For Bayesian analysis, information on the choice of priors and Markov chain Monte Carlo settings
- For hierarchical and complex designs, identification of the appropriate level for tests and full reporting of outcomes
- Estimates of effect sizes (e.g. Cohen's  $d$ , Pearson's  $r$ ), indicating how they were calculated

*Our web collection on [statistics for biologists](#) contains articles on many of the points above.*

### Software and code

Policy information about [availability of computer code](#)

Data collection

Data were matched to intrinsic brain networks and visualized using the freely-available iELVis software package and Matlab R2017b.

Data analysis

Data were matched to intrinsic brain networks and visualized using the freely-available iELVis software package and Matlab R2017b.

For manuscripts utilizing custom algorithms or software that are central to the research but not yet described in published literature, software must be made available to editors/reviewers. We strongly encourage code deposition in a community repository (e.g. GitHub). See the Nature Research [guidelines for submitting code & software](#) for further information.

### Data

Policy information about [availability of data](#)

All manuscripts must include a [data availability statement](#). This statement should provide the following information, where applicable:

- Accession codes, unique identifiers, or web links for publicly available datasets
- A list of figures that have associated raw data
- A description of any restrictions on data availability

The data supporting the results of this study are available from the corresponding authors upon reasonable request.

### Field-specific reporting

Please select the one below that is the best fit for your research. If you are not sure, read the appropriate sections before making your selection.

- Life sciences       Behavioural & social sciences       Ecological, evolutionary & environmental sciences

For a reference copy of the document with all sections, see [nature.com/documents/nr-reporting-summary-flat.pdf](https://www.nature.com/documents/nr-reporting-summary-flat.pdf)

## Behavioural & social sciences study design

All studies must disclose on these points even when the disclosure is negative.

Study description	The data are a mix of quantitative network and intracranial stimulation parameters and first-person reports following brain stimulation.
Research sample	The sample comprised 67 neurosurgical patients at the Stanford Hospital tested between 2008 and 2018.
Sampling strategy	The sample was a 'convenience' sample of inpatients being treated at the Stanford Hospital. Every effort was made to include data from any relevant patients over the past 10 years, including consideration of 119 patients. Ultimately 67 patients were included as having data relevant to the present study, with >1500 unique intracranial electrodes.
Data collection	Data were collected using intracranial EEG as well as simultaneous video recordings and supplemental handwritten notes of effects elicited with stimulation. Typically only the participant and researcher(s) were present, although nursing staff occasionally entered the room for necessary procedures. Both experimenter and patient were blind to the aims of the study, as the study is a retrospective assessment of a decade of data and was not envisioned beforehand.
Timing	Patients were investigated between 2008 and 2018.
Data exclusions	The main relevant exclusions were of pathological electrode channels showing epileptiform activity, which were never considered for analysis. Additionally, electrodes that fell outside brain network templates used in our analysis were not included in our analysis. Patients were excluded based only on practical considerations (lacking stimulation sessions, lacking MRI brain scans, etc.).
Non-participation	No participants dropped out/declined participation.
Randomization	Patients were not assigned to groups, but rather data from all patients was pooled, and global trends across all patients were investigated.

## Reporting for specific materials, systems and methods

We require information from authors about some types of materials, experimental systems and methods used in many studies. Here, indicate whether each material, system or method listed is relevant to your study. If you are not sure if a list item applies to your research, read the appropriate section before selecting a response.

### Materials & experimental systems

n/a	Involvement in the study
<input checked="" type="checkbox"/>	<input type="checkbox"/> Antibodies
<input checked="" type="checkbox"/>	<input type="checkbox"/> Eukaryotic cell lines
<input checked="" type="checkbox"/>	<input type="checkbox"/> Palaeontology
<input checked="" type="checkbox"/>	<input type="checkbox"/> Animals and other organisms
<input type="checkbox"/>	<input checked="" type="checkbox"/> Human research participants
<input checked="" type="checkbox"/>	<input type="checkbox"/> Clinical data

### Methods

n/a	Involvement in the study
<input checked="" type="checkbox"/>	<input type="checkbox"/> ChIP-seq
<input checked="" type="checkbox"/>	<input type="checkbox"/> Flow cytometry
<input type="checkbox"/>	<input checked="" type="checkbox"/> MRI-based neuroimaging

## Human research participants

Policy information about [studies involving human research participants](#)

Population characteristics	See above. Epilepsy affects sexes and races roughly equally and our sample was consistent with this.
Recruitment	See above. Data were gathered as part of a routine clinical mapping electrical stimulation procedure conducted with all epilepsy patients in the neurosurgical inpatient unit.
Ethics oversight	The study was approved by the Stanford Institutional Review Board for human participants research.

Note that full information on the approval of the study protocol must also be provided in the manuscript.

## Magnetic resonance imaging

### Experimental design

Design type	Only morphometric (structural/anatomical) scans were used in this study.
Design specifications	n/a

Behavioral performance measures

n/a

## Acquisition

Imaging type(s)

Structural

Field strength

3.0 Tesla

Sequence &amp; imaging parameters

T1-weighted scan: 256 x 256 matrix, 186 slices, 0.90 x 0.90 x 0.90 mm voxels, 240 mm field-of-view, 7.60 ms TR; SPGR sequence.

Area of acquisition

Whole-brain scan

Diffusion MRI

 Used Not used

## Preprocessing

Preprocessing software

Segmentation of T1 scans and cortical surface reconstructions using Freesurfer v6.0.

Normalization

Data were normalized to MNI space for global analyses using a non-linear transform.

Normalization template

The 'fsaverage6' template in Freesurfer v6.0.

Noise and artifact removal

n/a as our scans were not functional MRI.

Volume censoring

n/a as our scans were not functional MRI.

## Statistical modeling & inference

Model type and settings

n/a

Effect(s) tested

n/a

Specify type of analysis:

 Whole brain  ROI-based  BothStatistic type for inference  
(See [Eklund et al. 2016](#))

Correlation coefficients and regression coefficients (not used directly with MRI data; individual patient MRI scans were instead used to assign electrodes to specific brain regions and intrinsic networks in subject-specific space).

Correction

n/a to our analyses

## Models & analysis

n/a | Involved in the study

  Functional and/or effective connectivity  Graph analysis  Multivariate modeling or predictive analysis